1987

Vertical wind shear as a predictor of tropical cyclone motion.

Meanor, Denis H.

NAVAL POSTGRADUATE SCHOOL
Monterey, California

THESIS

VERTICAL WIND SHEAR AS A PREDICTOR
OF TROPICAL CYCLONE MOTION

by

Denis H. Meanor

March 1987

Thesis Advisor R. L. Elsberry

UNCLASSIFIED
SECURITY CLASSIFICATION OF THIS PAGE

REPORT DOCUMENTATION PAGE

1a REPORT SECURITY CLASSIFICATION NCLASSIFIED	1b RESTRICTIVE MARKINGS
2a SECURITY CLASSIFICATION AUTHORITY	3 DISTRIBUTION/AVAILABILITY OF REPORT Approved for public release; distribution unlimited
2b DECLASSIFICATION/DOWNGRADING SCHEDULE	
4 PERFORMING ORGANIZATION REPORT NUMBER(S)	5 MONITORING ORGANIZATION REPORT NUMBER(S)
6a NAME OF PERFORMING ORGANIZATION aval Postgraduate School	6b OFFICE SYMBOL (If applicable) 63
7a NAME OF MONITORING ORGANIZATION Naval Postgraduate School	
6c ADDRESS (City, State, and ZIP Code) onterey, California 93943-5000	7b ADDRESS (City, State, and ZIP Code) Monterey, California 93943-5000
8a NAME OF FUNDING/SPONSORING ORGANIZATION	8b OFFICE SYMBOL (If applicable)
9 PROCUREMENT INSTRUMENT IDENTIFICATION NUMBER	
8c ADDRESS (City, State, and ZIP Code)	10 SOURCE OF FUNDING NUMBERS PROGRAM ELEMENT NO / PROJECT NO / TASK NO / WORK UNIT ACCESSION NO

11 TITLE (Include Security Classification)
ERTICAL WIND SHEAR AS A PREDICTOR OF TROPICAL CYCLONE MOTION

12 PERSONAL AUTHOR(S)
eanor, Denis H.

13a TYPE OF REPORT	13b TIME COVERED	14 DATE OF REPORT (Year Month Day)	15 PAGE COUNT
aster's Thesis	FROM ____ TO ____	1987 March	75

16 SUPPLEMENTARY NOTATION

17 COSATI CODES			18 SUBJECT TERMS (Continue on reverse if necessary and identify by block number)
FIELD	GROUP	SUB-GROUP	Tropical cyclone forecasting, wind shear, tropical cyclone motion, OTCM, decision tree, typhoons, forecast error, empirical orthogonal function analysis

19 ABSTRACT (Continue on reverse if necessary and identify by block number)

The effects of vertical wind shear in the environment on tropical cyclone motion are investigated for 1357 western North Pacific Ocean cases. An empirical orthogonal function analysis is used to represent the vertical shear of the zonal and meridional components between the 700, 400 and 250 mb levels. Composite wind-shear fields are developed for five past-motion storm categories and analyzed to determine their statistical differences. The significant differences between these categories represents differing synoptic forcing by the wind shear that affects storm motion. Within the category of storms moving northwest, significant differences occur between right- and left-turning cyclones. This demonstrates that the vertical shears derived from operationally analyzed wind fields contain synoptic forcing information that is revelant to tropical cyclone motion. A regression analysis is used to

20 DISTRIBUTION/AVAILABILITY OF ABSTRACT ☒ UNCLASSIFIED/UNLIMITED ☐ SAME AS RPT ☐ DTIC USERS	21 ABSTRACT SECURITY CLASSIFICATION Unclassified
22a NAME OF RESPONSIBLE INDIVIDUAL Russell L. Elsberry	22b TELEPHONE (Include Area Code) 408-646-2373 / 22c OFFICE SYMBOL 63Es

D FORM 1473, 84 MAR 83 APR edition may be used until exhausted
All other editions are obsolete

SECURITY CLASSIFICATION OF THIS PAGE
UNCLASSIFIED

Block 19 (continued)

identify potential predictors from among the wind-shear EOF coefficients. These predictors are included in the regression equations to post-preocess the 24-, 48- and 72-h OTCM forecasts for 1982-1983. The modified OTCM tracks utilizing this scheme have an average error of 419 km at 72 h, which is an improvement of 174 and 212 km over the unmodified OTCM and official JTWC 72-h forecast errors, respectively. Wind-shear EOF coefficients included in a decision tree to select the best objective forecast aid only nominally increased the accuracy of the "optimum" forecasts.

Approved for public release; distribution is unlimited.

Vertical Wind Shear as a Predictor of Tropical Cyclone Motion

by

Denis H. Meanor
Lieutenant Commander, United States Navy
B.A., Miami University, 1976

Submitted in partial fulfillment of the
requirements for the degree of

MASTER OF SCIENCE IN METEOROLOGY AND OCEANOGRAPHY

from the

NAVAL POSTGRADUATE SCHOOL
March 1987

ABSTRACT

The effects of vertical wind shear in the environment on tropical cyclone motion are investigated for 1357 western North Pacific Ocean cases. An empirical orthogonal function analysis is used to represent the vertical shear of the zonal and meridional components between the 700, 400 and 250 mb levels. Composite wind-shear fields are developed for five past-motion storm categories and analyzed to determine their statistical differences. The significant differences between these categories represents differing synoptic forcing by the wind shear that affects storm motion. Within the category of storms moving northwest, significant differences occur between right- and left-turning cyclones. This demonstrates that the vertical shears derived from operationally analyzed wind fields contain synoptic forcing information that is revelant to tropical cyclone motion. A regression analysis is used to identify potential predictors from among the wind-shear EOF coefficients. These predictors are included in regression equations to post-process the 24-, 48- and 72-h OTCM forecasts for 1982-1983. The modified OTCM tracks utilizing this scheme have an average error of 419 km at 72 h, which is an improvement of 174 and 212 km over the unmodified OTCM and official JTWC 72-h forecast errors, respectively. Wind-shear EOF coefficients included in a decision tree to select the best objective forecast aid only nominally increase the accuracy of the "optimum" forecasts.

TABLE OF CONTENTS

LIST OF FIGURES

ACKNOWLEDGEMENTS

The completion of this study was made possible by the generous assistance of many individuals. I wish to thank Dr. Russell Elsberry who directed this research effort. His interest in this topic has motivated me to keep pressing on. The guidance he gave throughout this time was invaluable and taught me that large problems are best overcome one step at a time. I am grateful to Mr. Jim Peak for the continuous assistance he provided in tackling the computer problems associated with this work. His patience and willingness to take time to help me in each step has been much appreciated. I would like to thank Dr. C.-P. Chang, my second reader, for his insightful comments which contributed to a better thesis.

I would like to thank Dr. Ted Tsui, Naval Environmental Prediction Research Facility, for preparing the comprehensive data sets used in this study. Lt. William Wilson and Capt. Thomas Schott accomplished the initial wind EOF analysis that was the foundation on which this work was built. The facilities and personnel at the W. R. Church computer center provided the computing and consulting resources for this study.

Finally, I thank my wife, Elizabeth, for her unending love, support and encouragement these two years while my thoughts were often on my graduate studies. This thesis has been completed as a result of her efforts in ways too numerous to count.

I. INTRODUCTION

A. BACKGROUND

The western North Pacific Ocean is the most active tropical cyclone basin in the world. During the 25-year period ending in 1984, an annual average of 31 tropical cyclones occurred (NAVOCEANCOMCEN/JTWC, 1984). The need for accurate storm forecasts is of utmost importance to the civilian and military communities. The loss of both life and property from these storms can be considerable. To minimize the amount of damage caused by these severe storms and to provide more accurate warnings to ships and shore facilities, the Commander U. S. Seventh Fleet has set the maximum forecast error requirement for tropical cyclones to be 50, 100 and 150 n mi for the 24-, 48- and 72-h forecasts, respectively. Responsibility for forecasting tropical cyclones in this region lies with the Joint Typhoon Warning Center (JTWC) in Guam. The Annual Tropical Cyclone Report (NAVOCEANCOMCEN/JTWC, 1984) lists the mean annual errors for these times since 1971 as 117, 233 and 363 n mi at 24, 48 and 72 h, respectively. To meet the above goal, forecast errors must be decreased by over 50 percent.

Development of tropical cyclone track prediction models has been underway for many years. These models generally fall into one of six categories under either the statistical or dynamical model headings (Neumann, 1985). The simplest statistical model is the analog approach, which relies on the repetitiveness of large-scale patterns and previous cyclone tracks. A historical search of the records is made to find similar storm tracks to use as guidance for the current storm. The HURRicane ANalog (HURRAN) developed by Hope and Neumann (1970) is still in use at the National Hurricane Center (NHC) in Coral Gables, FL. The first analog model used in the western North Pacific area was TYFOON (Hodge and McKay, 1970). TYAN is the current analog model used by JTWC.

Statistical regression models were developed due to the inability of the analog models to deal with anomalous storm tracks. The stepwise screening regression approach utilizes predictors that represent the climatology, persistence and the surrounding environmental flow (steering of the cyclone). The CLImatology and PERsistence (CLIPER) model for the western North Pacific area (Xu and Neumann,

1985) utilizes the present storm position and intensity, date and the present and past motion to predict the storm track to 72 h. The accuracy of the position of the storm at a warning time is critical. The CLIPER model is normally used as a benchmark to indicate the skill of other objective aids.

One of the weaknesses of the CLIPER model is that it does not consider the effect of the environmental flow on storm movement. The statistical-synoptic models include this information as predictors. The first objective technique utilizing synoptic forcing at the 500 mb level was developed by Riehl et al. (1956). Studies of the relationship between the tropical cyclone track and the environmental steering flow responsible for a cyclone track have been pursued by many authors (e.g. Renard, 1968; George and Gray, 1976; Chan and Gray, 1982; Dong and Neumann, 1986).

The environmental information regarding adjacent synoptic features has been represented in two ways. Geopotential height data on a grid positioned relative to the tropical cyclone has been used in the development of NHC67 and NHC72 synoptic models (Neumann and Pelissier, 1981). Another approach has been to represent the height data with empirical orthogonal function (EOF) coefficients (Shaffer and Elsberry, 1982; Shapiro and Neumann, 1984). A problem with using objectively-analyzed height fields in the tropics is that temperature gradients are weak and may not provide an accurate estimate of the height gradients (geostrophic or gradient winds). Chan (1985) used objectively-analyzed wind fields to demonstrate that the steering flow patterns based on these winds were similar to those based on composites of rawinsonde data. EOF representations of those wind fields and the associated synoptic forcing of tropical cyclone motion was the basis of the research by Wilson (1984) and Schott (1985).

The statistical-dynamic model uses the same predictors as in the statistical-synoptic models, as well as additional predictors of forecast fields that are provided by the numerical models. The NHC73 model is an example of this type of model and has proven to have the best performance in a comparison with five other objective aids in the Atlantic Ocean basin (Neumann and Lawrence, 1975). The MOdified HATRACK model (Renard et al., 1973) uses heavily smoothed isobaric height prognoses to obtain the steering field for the tropical cyclone.

There are two categories of dynamic (numerical) models: barotropic and baroclinic. Theoretically, these models should provide a better prediction of anomalous tracks since they more accurately describe dynamical processes resulting

from the interaction of the vortex with the environment. Barotropic models rely on vorticity advection as the primary mechanism for motion (Renard, 1968). The SANBAR model (Sanders and Burpee, 1968) is a barotropic model that predicts a cyclone track based on the location of the minimum stream function or maximum vorticity. Steering is provided by a deep-layer, pressure-weighted mean wind field. Estimates of this mean wind field are provided by using the 850, 500 and 250 mb level winds (Sanders et al., 1980). However, these models lack both a unique steering level and adequate treatment of the vortex-environmental interaction (Ley and Elsberry, 1976).

Baroclinic models are generally primitive equation models that predict motion based on the mesoscale horizontal interaction of the cyclone and its environment. The National Meteorological Center (NMC) Moveable Fine Mesh (MFM) model has a 60 km grid spacing and predicts storm motion based on the surface vorticity maximum (Hovermale et al., 1975). The Navy Nested Tropical Cyclone Model (NTCM), which was developed by Harrison (1973; 1981), is run to 72 h twice daily for Northern Hemisphere typhoons. In a test conducted by Harrison and Fiorino (1982), the NTCM was found to have considerable skill in path prediction beyond 36 h. The One-way Tropical Cyclone Model (OTCM) is a three-layer, primitive equation model (Hodur and Burk, 1978) that is currently in use at JTWC. It has proven to be one of the best of the eleven objective aids evaluated by Tsui (1984) and has been used as the primary guidance for storm forecasts (Fiorino, 1985; Elsberry and Peak, 1986).

The absence of upper-air wind observation stations in the Pacific Ocean area is the most serious hindrance to accurate initialization of the present numerical models. With the advent of jet aircraft, there has been an increase of data at the upper tropospheric levels and a loss of information at the most important steering levels in the mid troposphere (Sanders et al., 1980; Pike, 1985). Satellites have improved the accuracy of detecting and positioning a storm, and have increased the amount of wind information at the highest and lowest levels of the troposphere. However, there is still a long way to go to approach the required maximum forecast error goals.

No single objective aid has been found to be superior for all forecast situations (Jarrell et al., 1978; Tsui, 1984). To assist the Typhoon Duty Officer at JTWC in evaluating the multiple objective aids, a Combined Confidence Rating System (CCRS) has been developed by Tsui and Truschke (1985) that combines all the guidance methods based on the historical accuracy of the 72-h forecasts. However, this system

currently does not account for the consistency of a particular model output. Another method to aid the forecaster is the "decision-tree" approach of evaluating objective aids (Peak and Elsberry, 1985; 1987). In this method, selection of an optimum aid for a particular situation is through a series of yes/no decisions ("branches") based on past and present characteristics of a cyclone.

B. OBJECTIVES

Vertical wind shear has not previously been investigated as a predictor of tropical cyclone motion. The subject study will focus on this aspect of the storm environment. The data set of Wilson (1984) and Schott (1985) will be used in this study of western North Pacific Ocean tropical cyclones. In Chapter II, the mean zonal and meridional wind-shear fields for three shear layers will be analyzed and described. Empirical orthogonal functions (EOF) will be used to represent the synoptic forcing in these wind-shear fields, since this technique results in a substantial savings of computer storage space. In Chapter III, the storms will be divided into five categories based on the past 12-h speed and direction of motion. Composite mean wind-shear fields will be generated for each category and the statistical difference between the categories will be investigated. The objective is to demonstrate the differences in the synoptic forcing among the categories that determine the future storm track. Those storms that move to the northwest will be further subdivided into three categories and differences in the synoptic forcing will be compared among these categories.

A second objective of this study is to utilize the synoptic forcing information contained in the EOF coefficients to adjust the OTCM track similar to the approach of Schott (1985) and Schott et al. (1987). In Chapter IV, a stepwise regression analysis scheme based on storm-related EOF predictors will be applied in a "post-processing" scheme to reduce systematic errors in the OTCM forecasts. The third objective involves including the wind-shear EOF coefficients in a decision-tree algorithm (Peak and Elsberry, 1987) that selects objective aids based on synoptic and storm-related parameters. Chapter V will present the results of this method of improving forecast errors. Recommendations for future research in this area are included in Chapter VI.

II. DATA DESCRIPTION AND STUDY METHODS

A. DATA ACQUISITION AND FIELD DEFINITION

The wind fields in this study are the same sets used by Wilson (1984) and Schott (1985). The wind information for the western North Pacific area has been obtained from the Global Band Analysis (GBA) operationally generated at the U.S. Navy's Fleet Numerical Oceanography Center (FNOC). The GBA fields are plotted on a Mercator grid from 41°S to 59.8°N. The grid has a spacing of 2.5° longitude by 2.5° latitude at 22.5° N and S. The zonal and meridional wind fields are available from 00 GMT and 12 GMT at the surface, 700, 400, 250 and 200 mb. Surface data are from land observations and ship reports while upper-air data are based on rawinsonde observations, aircraft reports and satellite-derived cloud motion vectors. Temperature analyses at the intermediate levels are used to couple the winds at different vertical levels via the thermal wind relationship. The 12-h old analysis plus 5 % climatology is used as the first-guess field for the current analysis. If no observations are available in a region, the final analysis becomes the previous analysis adjusted towards climatology.

The Annual Tropical Cyclone reports published by the Joint Typhoon Warning Center (JTWC) from 1975-1983 were used to select the cases. Warning positions, best track information and intensity estimates are included at six-hour intervals. In addition, the 24-, 48- and 72-h official forecasts are given. The following restrictions apply to the selection of cases: 1) tropical storms must be located in the eastern hemisphere east of 100°E with a warning position less than 34.6°N; 2) storm intensity must be at least 18 m/s (35 kt); and 3) zonal and meridional wind components must have been available at the 700, 400 and 250 mb levels. A total of 1357 cases meet these requirements. By random selection, this set is reduced to 682 cases for computing the EOF coefficients due to the computer's central core limit.

The geographically-oriented grid of 527 points is the same as in Wilson (1984). These points are equidistant at 277.8 km. There are 31 east-west points and 17 north-south points. Thus, the domain is 8334 km by 4445 km. The grid center (row 9, column 16) is coincident with the tropical cyclone center in each case. The zonal and meridional component winds at the three levels were extracted by Wilson (1984) from the GBA and transferred to the grid by means of a bilinear interpolation scheme.

B. MEAN AND STANDARD DEVIATION FIELDS

The vertical wind shear fields are computed for the 682 cases by subtracting the wind component at the larger pressure (lower level) from the wind component at the smaller pressure (upper level). Thus, three shear fields (mid- and upper-tropospheric and deep layer) are created for the zonal and meridional components. Six combinations of upper minus lower level shear combinations are possible to produce the positive and negative shears of each gridpoint value (Table 1).

TABLE 1

Shear combinations that are possible to produce the shear values at each gridpoint.

Positive (Westerly or Southerly) Shear

1. Large Upper (W or S) - Small Lower (W or S)
2. Large Upper (W or S) - Small Lower (E or N)
3. Small Upper (E or N) - Large Lower (E or N)

Negative (Easterly or Northerly) Shear

4. Small Upper (W or S) - Large Lower (W or S)
5. Large Upper (E or N) - Small Lower (E or N)
6. Large Upper (E or N) - Small Lower (W or S)

The shear fields are normalized to 100 mb to eliminate biasing the shear values by variable depths of the layers. The patterns remain the same as before normalization, as only the magnitude of the shear changed (Figs. 2.1, 2.2). For both zonal and meridional components, the largest mean shear appears in the 250-400 mb layer, with values about 50% greater than in the deep layer and 75% greater than in the 400-700 mb layer. The largest variance is also in the upper layer rather than in the deep or lower layers.

Each of the zonal shear patterns in Figs. 2.1a, 2.3a and 2.5a has positive (westerly) shear to the north where the upper-level westerlies are stronger than the low-level westerlies. Shear is negative (easterly) to the south in regions with upper-level easterlies over low-level equatorial westerlies where the monsoonal trough is displaced away from the equator. The line that runs through the cyclone center (dot) is

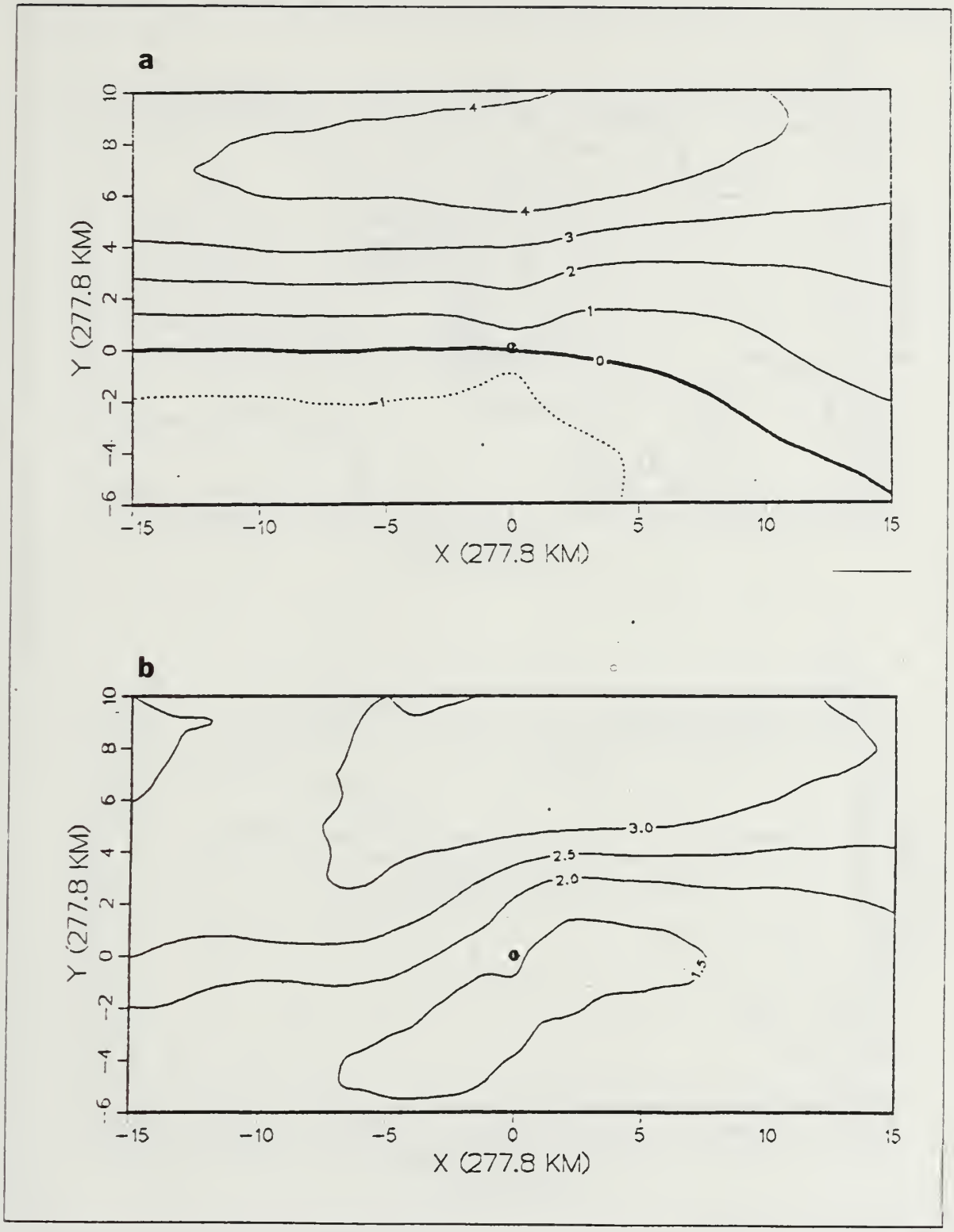

Figure 2.1 (a) Mean and (b) standard deviations of the U-component shear (m/s per 100 mb) for the 400-700 layer.

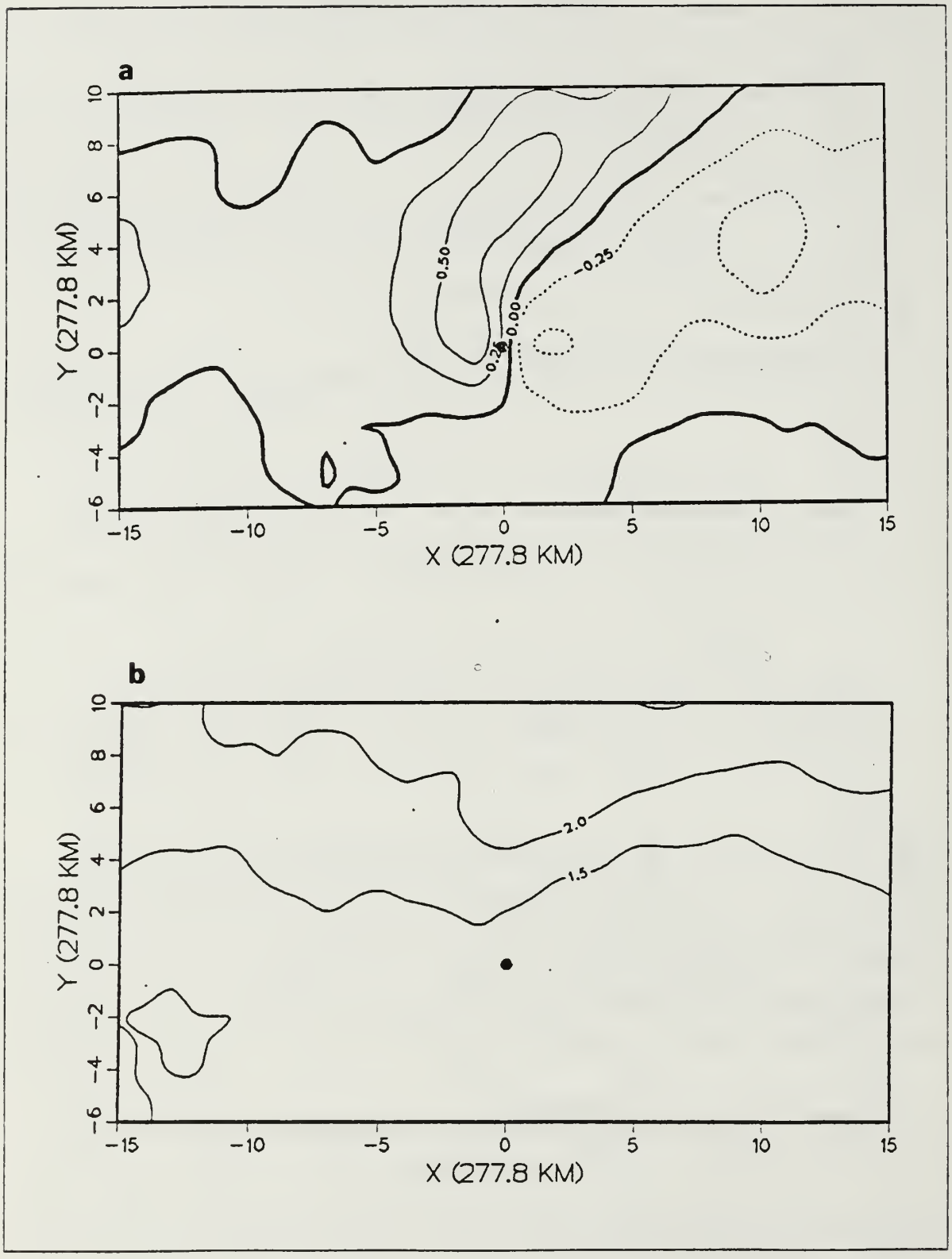

Figure 2.2 As in Fig. 2.1, except for V-component.

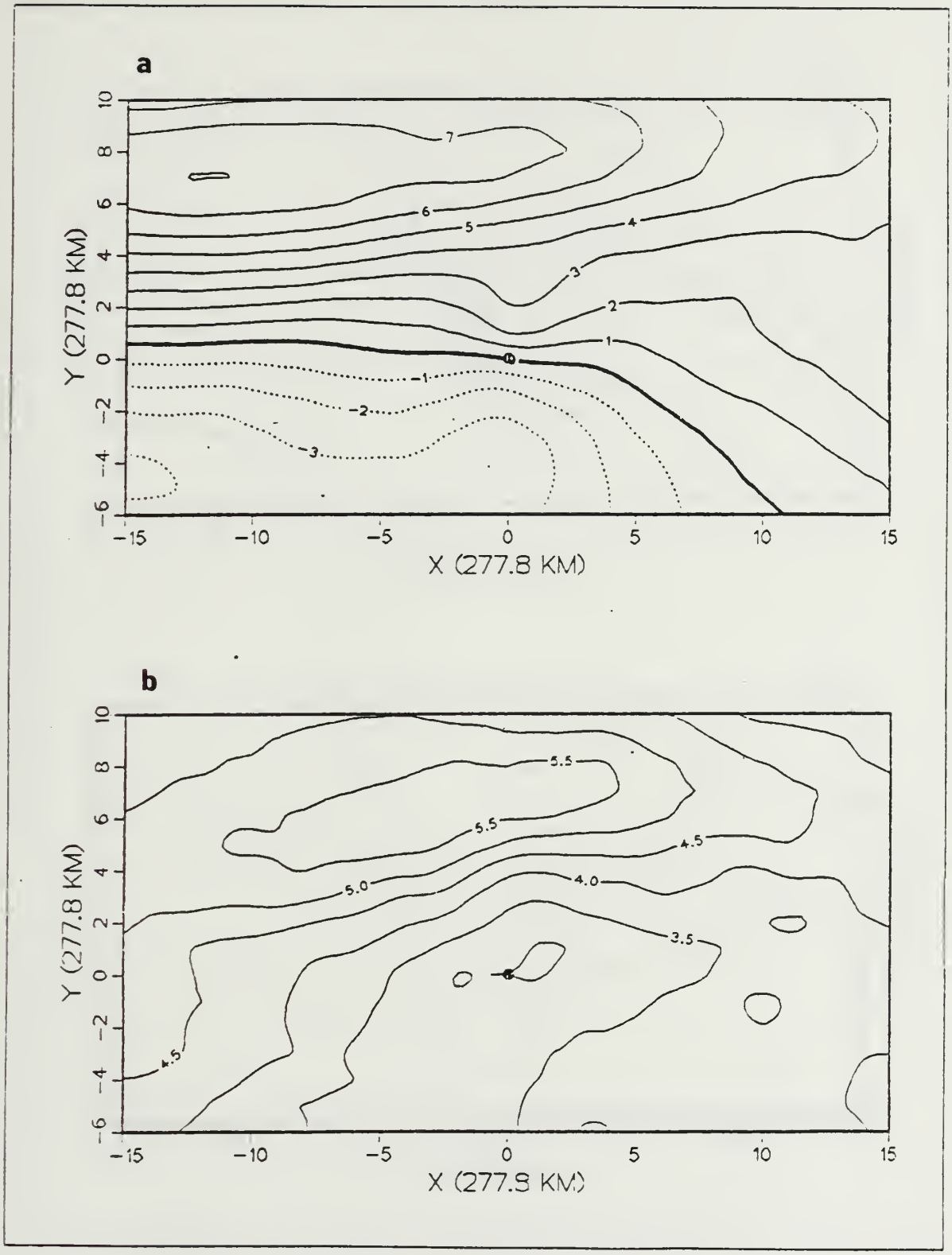

Figure 2.3 As in Fig. 2.1, except for 250-400 mb layer.

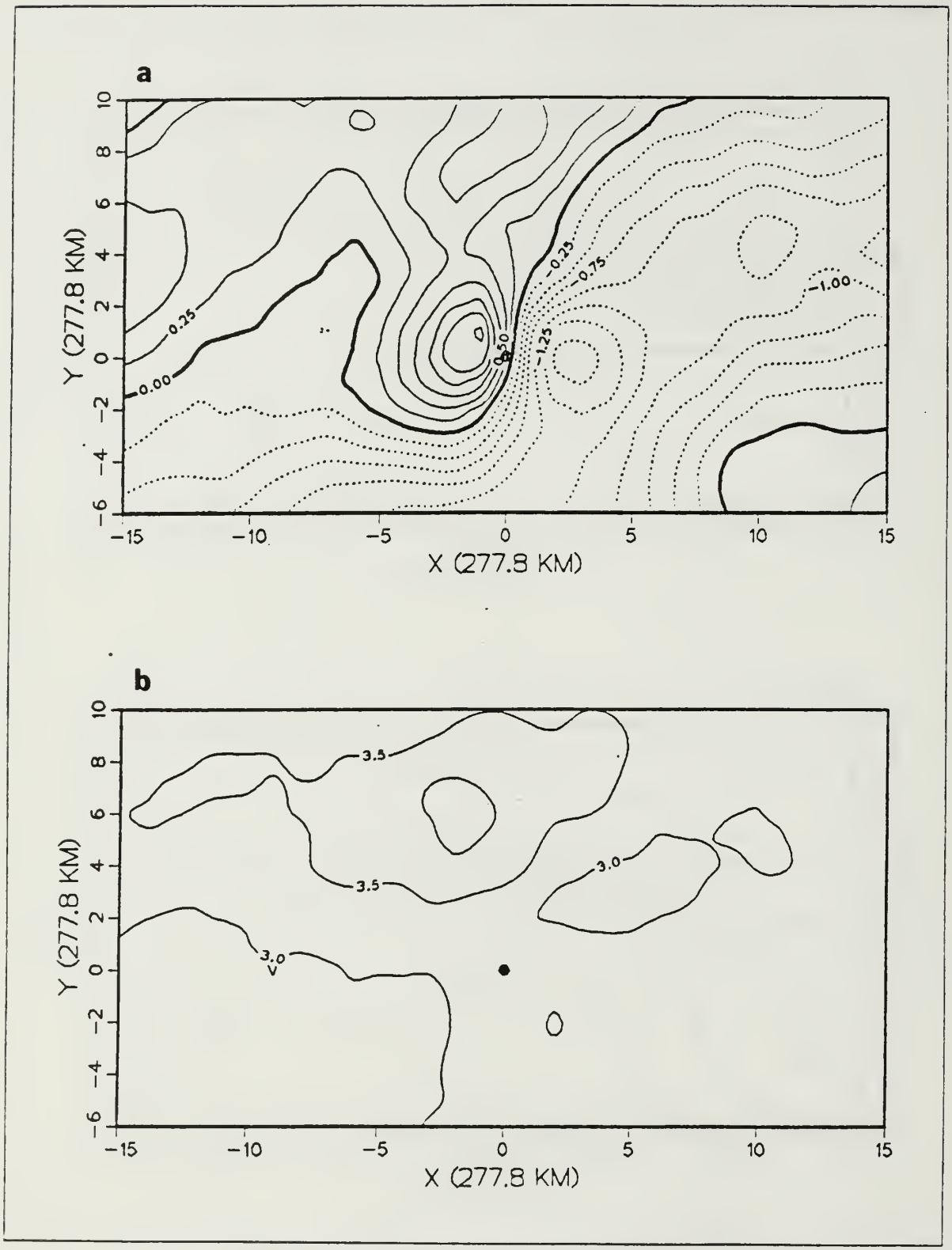

Figure 2.4 As in Fig. 2.3, except for V-component.

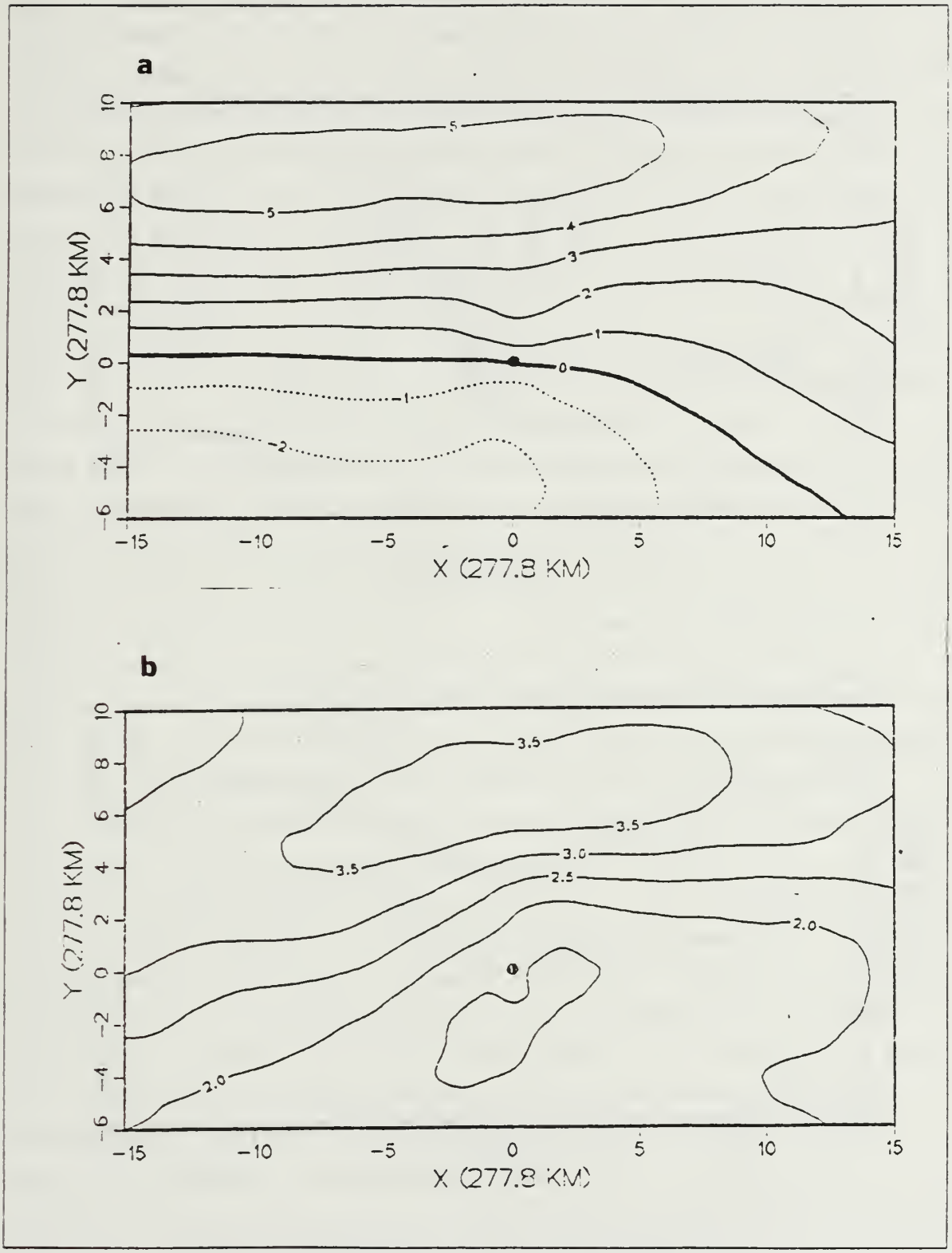

Figure 2.5 As in Fig. 2.1, except for 250-700 mb shear layer.

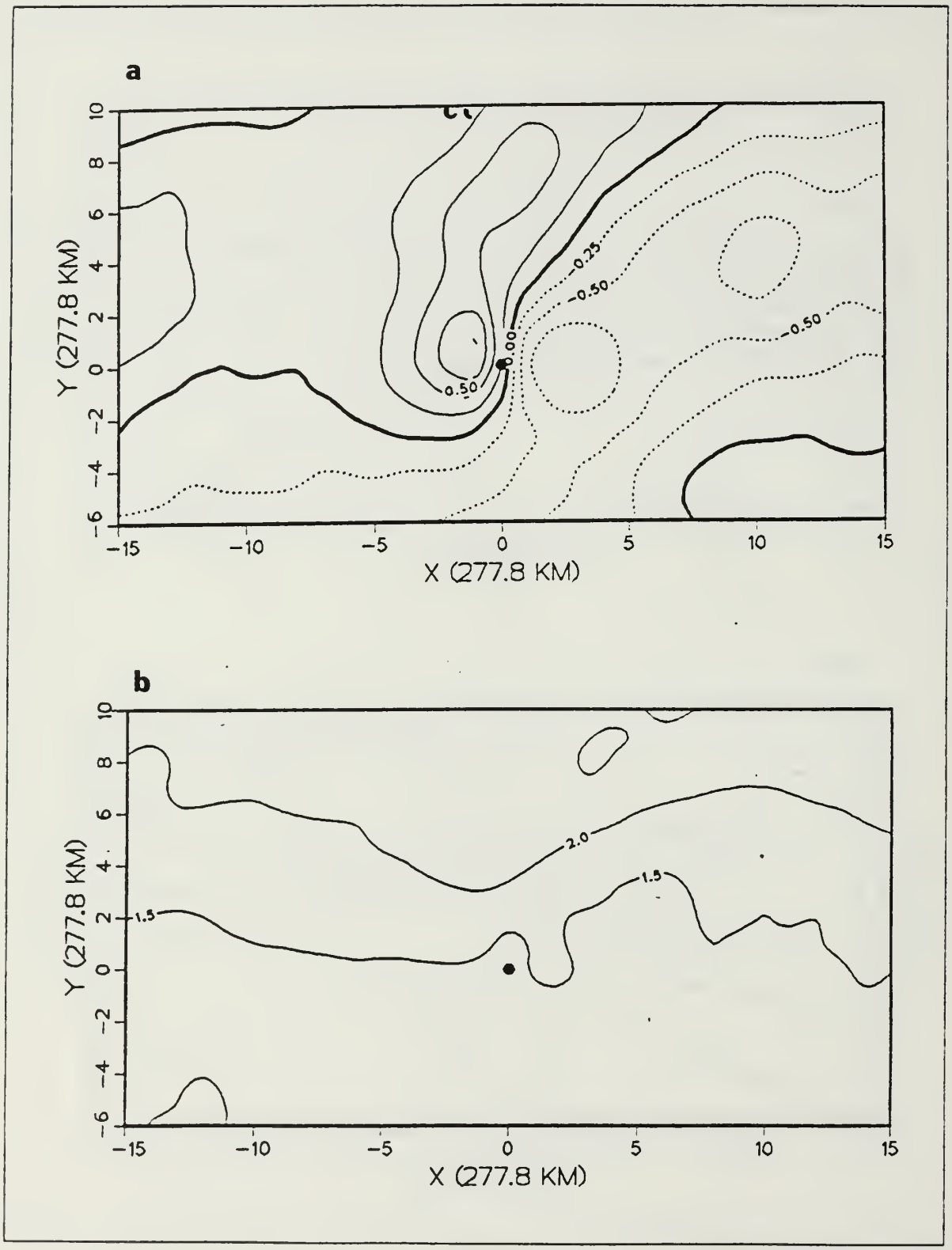

Figure 2.6 As in Fig. 2.5, except for V-component.

indicative of no vertical zonal wind shear over the center, which is expected for tropical cyclone formation (Gray, 1979). In each case, the zero shear line trails off to the southeast behind the storm, which could be associated with the equatorward displacement of the inter-tropical convergence zone (ITCZ) farther east. The similarity of the zonal shear patterns in these layers reflects a similarity in the mean north-south temperature gradient at all levels. However, this similarity may not exist for individual cases. The largest mean vertical shear is in the upper layer (250-400 mb; Fig 2.3a), with the next largest shear in the deep layer (Fig. 2.5a). The smaller vertical shear in the lower troposphere is consistent with the fact that the lower troposphere in the tropics is conditionally unstable and does not support large baroclinicity. The standard deviation fields for the zonal components (Figs. 2.1b, 2.3b and 2.5b) all have increasing variability in the shear to the north of the cyclone, with the largest variability in the upper layer. It is interesting that the standard deviations are greater than the mean shear at nearly all points, so a large number of negative values can be expected in individual cases even though the overall mean value is positive.

In the mean meridional shear patterns (Figs. 2.2a, 2.4a and 2.6a), the shear is negative (northerly) to the east and south of the cyclone center and positive (southerly) to the north and west. The deep-layer shear is only half as large as that of the upper layer and is slightly larger than the lower-layer shear. These mean meridional shears are smaller and the patterns are more complex than for the mean zonal shears. Therefore, these shear fields are more difficult to tie to the synoptic pattern. The primary zero line separating the major positive and negative shears is generally oriented northeast to southwest across each field and lies over the storm center, as expected. Again, the highest temperatures (minimum east-west temperature gradients) are aligned with the zero vertical wind shear line that passes through the storm center. The negative shear to the east is associated with weak upper-level southerlies (or northerlies) over stronger lower-level southerlies in the tropical cyclone. Farther to the east, a strong northerly wind overlies a weak northerly wind. To the west, the positive shear is due to weak southerlies overlying even smaller southerlies or northerlies. The standard deviation fields are shown in Figs. 2.2b, 2.4b and 2.6b. When normalized, the upper-layer variability is the largest of the three layers. Maximum meridional shear variability is to the north for these cases, although a nearly homogeneous distribution of variability occurs in the upper layer. Here, the standard deviations are much greater than the means. The high variability of positive and negative values is indicative of warm ridges and cold troughs moving by a point on the grid.

C. EMPIRICAL ORTHOGONAL FUNCTION ANALYSIS

The application of empirical orthogonal function analysis to geophysical fields was first made by Lorenz (1956). It has been regularly used since to explain the large variation in atmospheric fields based on a minimum number of eigenvectors.

The application of the EOF method in this study will follow that by Wilson (1984) and Schott (1985). From 682 cases of 527 gridpoints, a matrix (A) is created with the scalar (zonal and meridional) wind shear fields for each of the three layers. A normalized matrix (Z) is formed by subtracting the mean (B) and dividing by the standard deviation (S).

$$Z(i,j) = (A(i,j) - B(i,j)) / S(i) , \qquad (2.1)$$

where z(i,j) and a(i,j) are the elements of matrices Z and A respectively, and b and s are the mean and standard deviation of row i in matrix A. A symmetric correlation matrix (R) is formed as

$$R = Z'Z / n , \qquad (2.2)$$

where Z′ is the transpose of matrix Z and n is the number of cases (682). A particular vector e in m dimensions is defined and normalized to length 1 so that e′e = 1. The scalar quantity v, which is the correlation between vector e and matrix Z, then is defined by

$$v = e'Re. \qquad (2.3)$$

In matrix form, V = E′RE. Here, E is a 527x527 matrix of eigenvectors and V is a matrix of eigenvalues (v) found when

$$| R - VI | = 0 , \qquad (2.4)$$

where I is the identity matrix and 0 is the null vector. The empirical orthogonal functions are the eigenvectors in E computed from the correlation matrix R. Each eigenvector e is associated with an eigenvalue v_i that accounts for a certain percentage of the variance in the field. The first eigenvector v_1 explains the largest percentage of

the total variance. Summing all the eigenvalues would account for 100% of the variance.

Any case in the normalized matrix Z can be reproduced once the EOF coefficients are known by computing

$$C = E'Z, \tag{2.5}$$

where C is a 527 x 682 orthogonal matrix of coefficients. Each column of C is a vector that corresponds to a particular case in Z and is reconstructed by

$$Z = CE. \tag{2.6}$$

The jth case of Z is approximated by a linear summation of eigenvectors and orthogonal coefficients

$$z(i,j) = \sum e(i)\, c(i,j) \quad j = 1,2,...,527. \tag{2.7}$$

By using the EOF method, a large percentage of the variance in a data field can be described with a relatively few eigenvectors. This is advantageous in the reduction of computer storage when the synoptic fields are represented on many gridpoints.

The eigenvectors in E are ranked in order of decreasing variance. Various approaches may be used to select a small set of vectors that must be retained to best describe the signal in the field. These methods have been reviewed in Shaffer and Elsberry (1982) and Wilson (1984). The Monte Carlo approach described by Preisendorfer and Barnett (1977) will be used to distinguish between vectors with signal and those with noise. The method involves generating 100 random data fields of standard normal deviates, which are then placed in a Z matrix. These represent purely random processes. The means and standard deviations are determined and the eigenvalues are calculated as described above for the shear values. Finally, the eigenvalues for the true physical data are compared with those from the random fields. The eigenvalues of the physical fields that differ from the means of the random field by more than two standard deviations are considered true signals that are significant at the 95 % confidence level. Those within two standard deviations of the means of the random field are considered to be noise and are not kept. A plot of the eigenvalues for

the 400-700 mb zonal shear fields vector versus the number of modes is shown in Fig. 2.7. As a result of this Monte Carlo selection process for each field, the largest number of modes selected to represent signal is 25 eigenvalues for the zonal fields and 35 eigenvalues for the meridional fields. A summary of the percentage of variance explained by retaining this number of modes appears in Table 2. Up to 88 % of the actual field is contained in only 25 zonal modes. In every case, the zonal shear field may be represented by at least ten fewer modes even though greater explained variance is achieved. Additionally, the deep layer is best represented, since a larger total percentage of the actual field can be reproduced even when the smallest number of modes are retained.

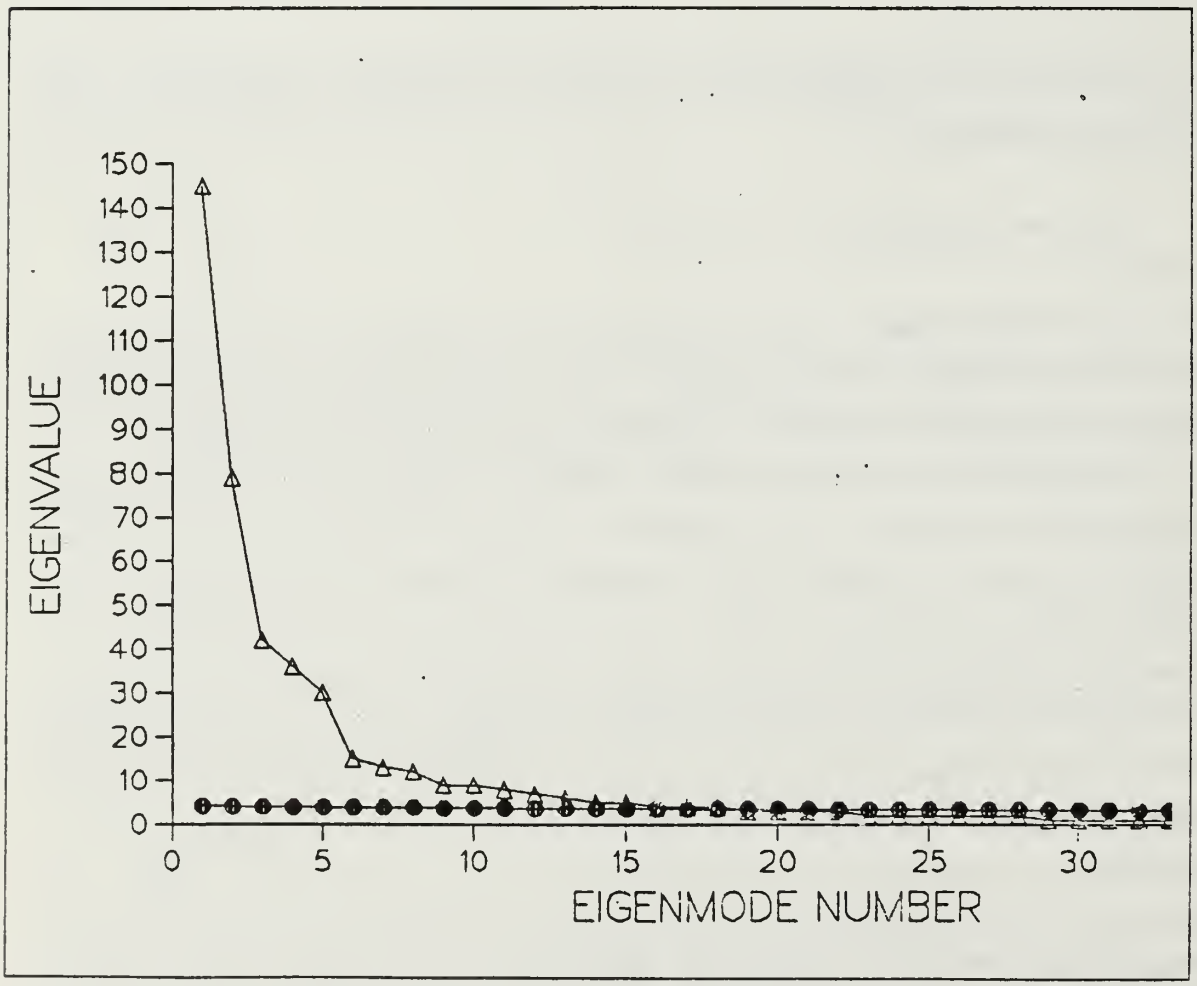

Figure 2.7 Eigenvalues for the 400-700 mb zonal shear (triangles) and the Monte Carlo eigenvalues plus two sigma (circles).

TABLE 2

The percent of variance explained by retaining 25 zonal and 35 meridional modes.

LAYER	ZONAL	MERIDIONAL
400 - 700 mb	85.0	79.9
250 - 400 mb	79.6	79.2
250 - 700 mb	88.4	84.0

Another interpretation of the values in Table 2 is that the amount of noise present as unexplained variance is as great as 21 % for the meridional and 20 % for the zonal shear components. Some of this noise may arise from erroneous observations. However, a large fraction is due to the sparse data distribution and the way in which the objective analysis method extrapolates into the data gap regions.

D. RESULTANT EMPIRICAL ORTHOGONAL FUNCTIONS

The 250-700 mb zonal shear eigenvectors 1 and 2 are plotted in Fig. 2.8a and 2.8b. In mode 1, which accounts for 27 % of the variance, the entire field is dominated by negative (easterly) shear that increases just to the north and west of the cyclone center. The opposite (westerly) shear can be represented by multiplying the eigenvalues by negative 1. The second mode explains 16 % and has negative (positive) shear to the north (south) of the mean location of the subtropical ridge in the original mean zonal wind fields of Wilson (1984). The eigenvectors for the other two layers are very similar in magnitude and pattern to these eigenvectors, which is also true for the third and fourth modes.

Mode 1 of the meridional pattern for the 250-700 mb layer (Fig. 2.9a) is also dominated by negative (northerly) shear over the field, except in the northwest corner and eastern central region. Only 11 % of the variance is explained by this mode. Although the upper-layer pattern is very similar to this deep-layer mean pattern, the first mode of the lower-layer shear is quite different and alternates between positive and negative shear regions oriented north-south. Eigenvector 2 patterns for all three layers are very similar to the deep-layer mode (Fig. 2.9b) and account for six to eight percent of the variance. Such a pattern could represent the vertical shears associated with alternating cold troughs and warm ridges to the north of the tropical cyclone.

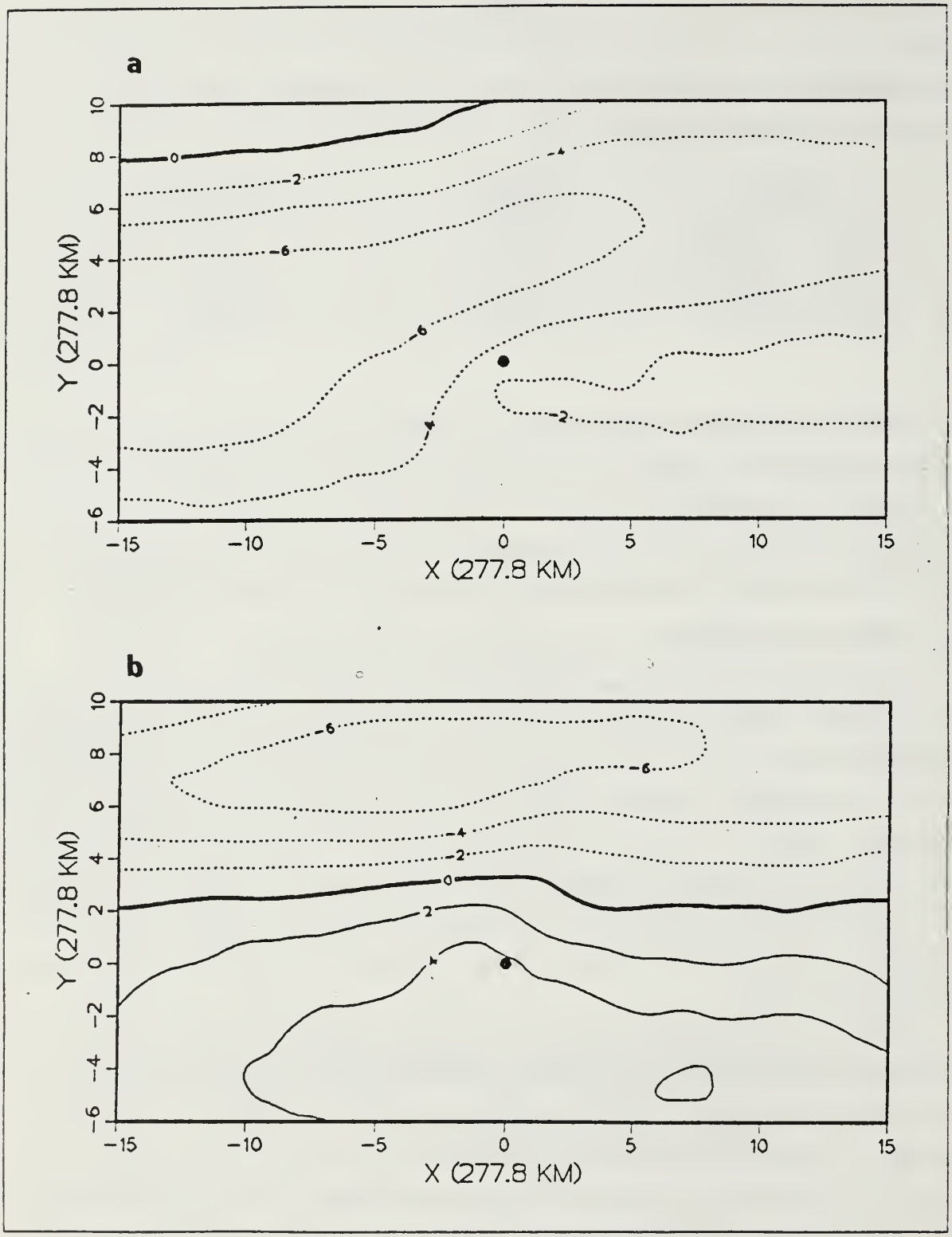

Figure 2.8 (a) Mode 1 and (b) mode 2 for the 250-700 mb zonal shear (normalized fields multiplied by 100).

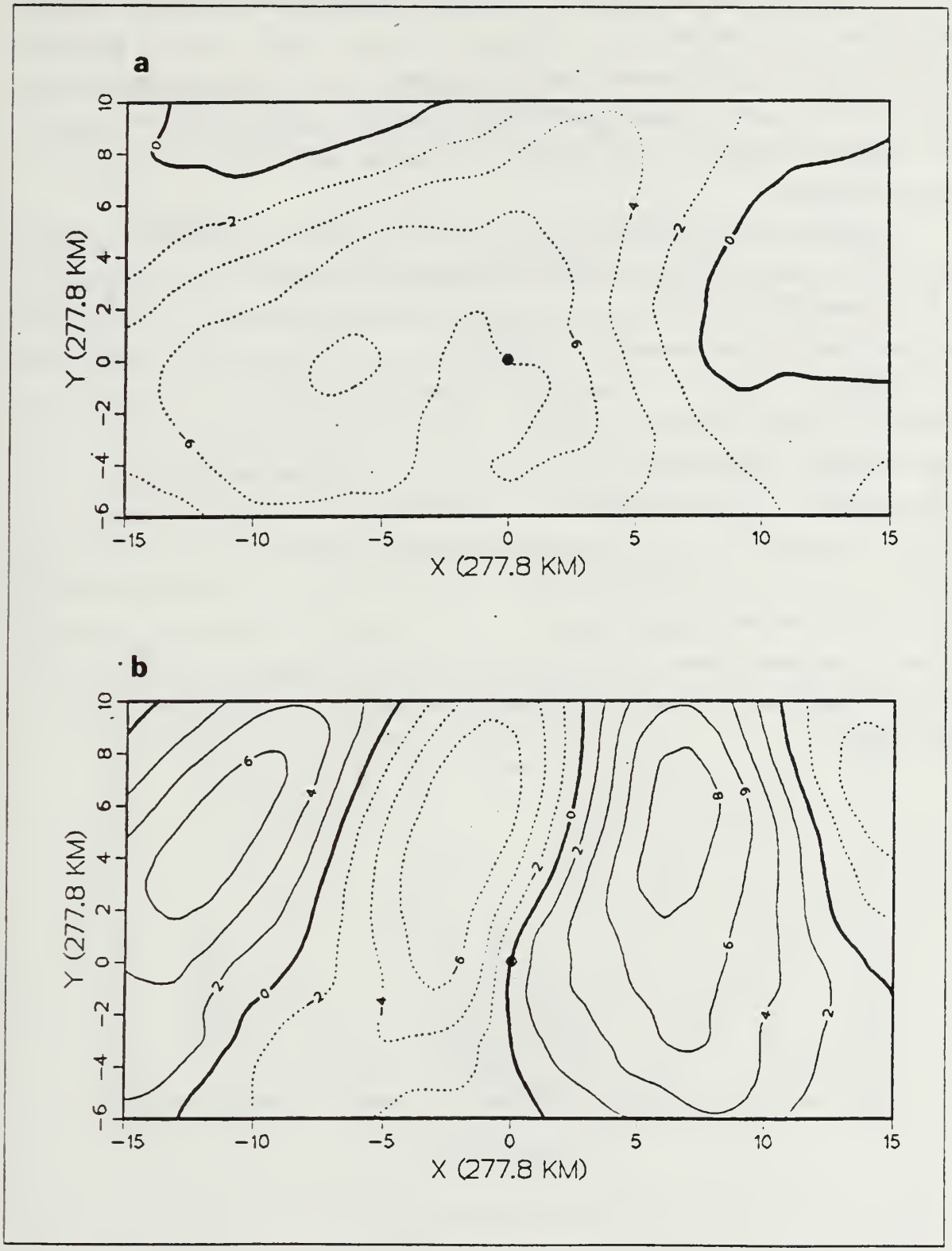

Figure 2.9 As Fig. 2.8 except for meridional shear modes.

Interpretation of the modes as observable atmospheric patterns is difficult because there are numerous shear combinations possible (Table 1). This is especially true for higher order eigenvectors in which the spatial patterns are more complex than modes 1 and 2. Large regions may contain a variety of signals that can be described by a particular eigenvector even though those signals may actually be a result of different processes.

Verification that the small number of modes retained does actually represent much of the original data field demonstrates the validity of using the EOF method. If all 527 eigenvectors are used, the field would be completely restored, but no savings in computer storage would be realized. Reducing the data to 25 zonal and 35 meridional modes realizes 95 % and 93 % savings in storage, respectively. The case chosen for validation is Typhoon Hope on 00 GMT 30 July 1979 (Fig. 2.10). The 400-700 mb zonal shear fields reconstituted by summing only 5 or 25 eigenvectors are shown in Fig. 2.11a and Fig. 2.11b, and represent 53 % and 85 % of the variance, respectively. Figures 2.12a and 2.12b are the corresponding 400-700 mb meridional shear fields using 5 and 35 eigenvectors and represent 30 % and 79 % of the variance respectively. These illustrations demonstrate that even a few modes can approximate the gross features of the shear pattern. Many of the smaller scale features in Fig. 2.10 may actually represent noise or unrepresentative values in the wind analyses of the data-sparse tropics.

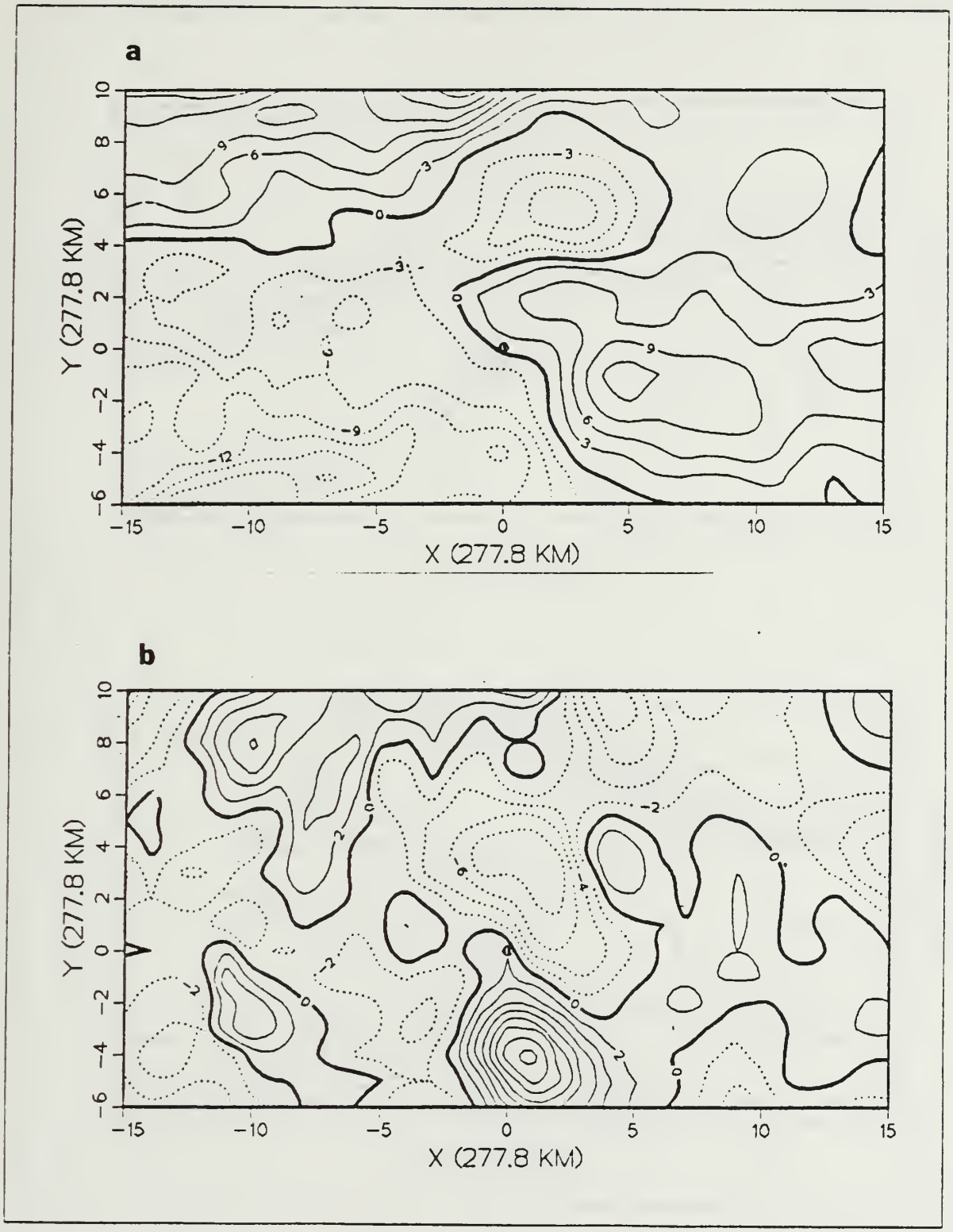

Figure 2.10 Original 400-700 mb (a) zonal and (b) meridional shear from Typhoon Hope on 00 GMT 30 July 1979.

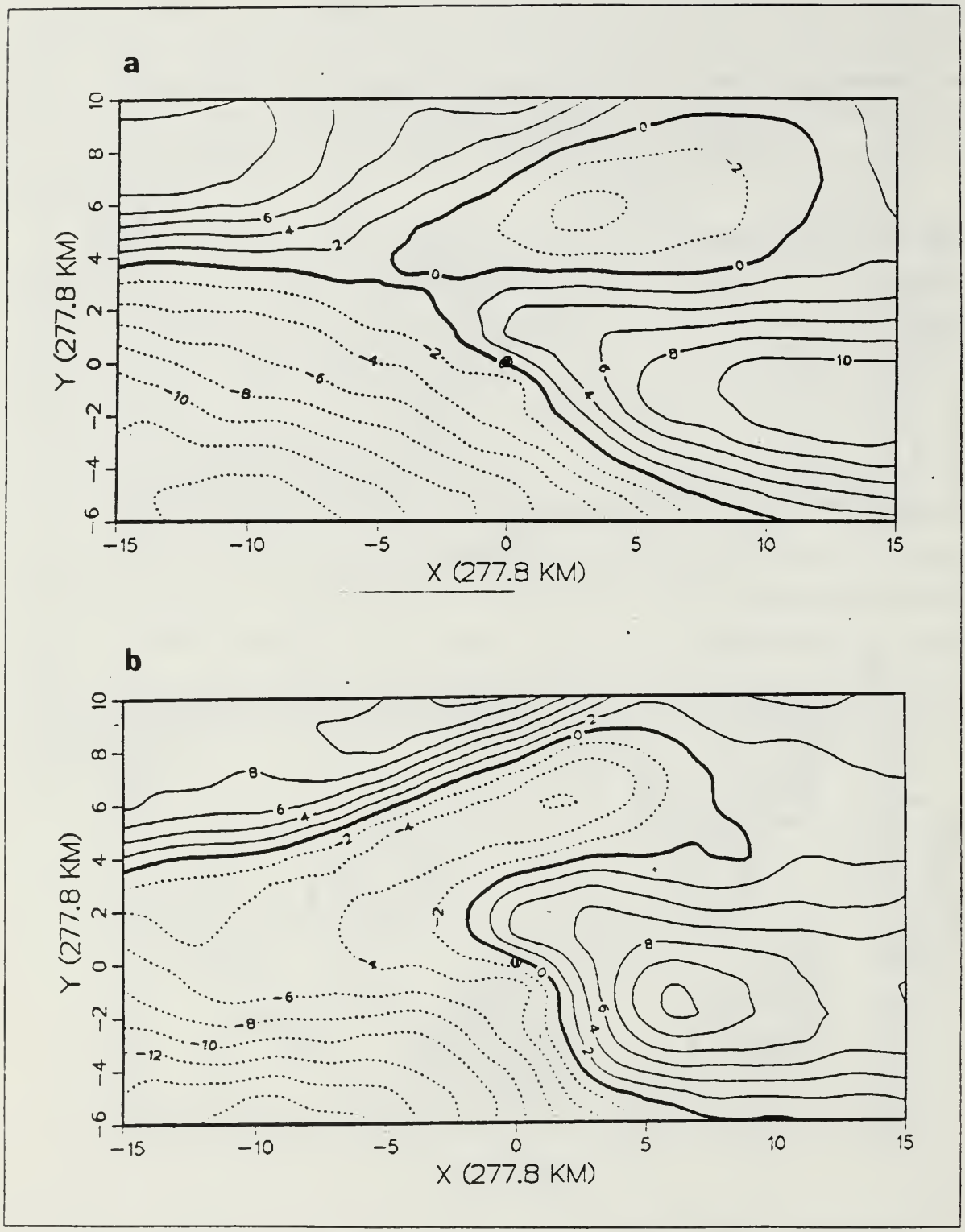

Figure 2.11 Reconstruction of the 400-700 mb zonal shear of Typhoon Hope using (a) only 5 and (b) only 25 eigenvectors.

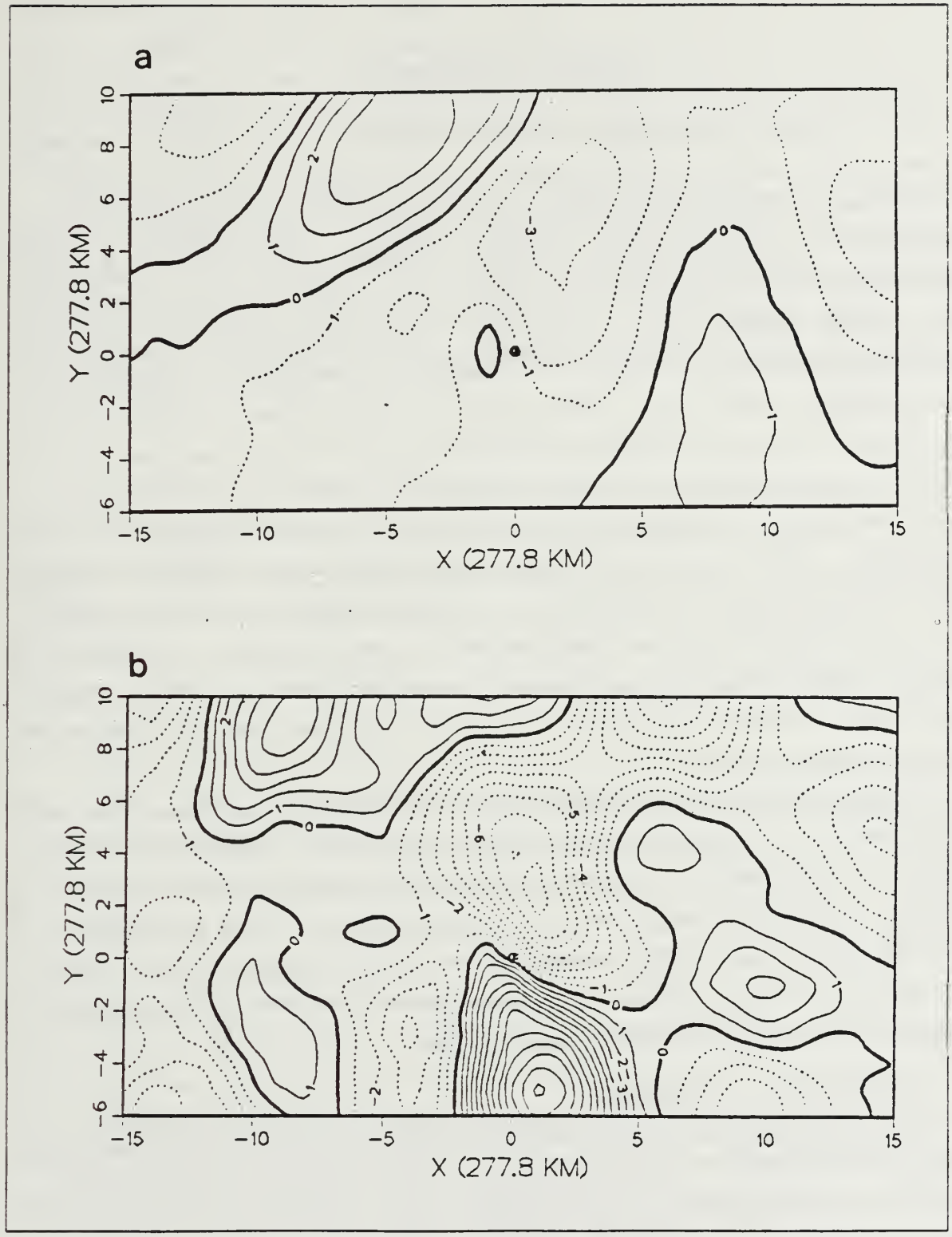

Figure 2.12 As in Fig. 2.11, except for meridional shear using (a) only 5 and (b) 35 eigenvectors.

III. DATA ANALYSIS

The usefulness of describing wind shear around the environment of tropical cyclones by EOF analysis was demonstrated in the last chapter. To further investigate the influence of wind shear on storm motion, the cases used in this study will be stratified to determine if the synoptic forcing is important. Recent studies of tropical track motion have been based on composites of the total wind field to represent the mean synoptic features in the environment. George and Gray (1976) used 13 stratification criteria in an attempt to best define the steering flows responsible for cyclone behavior. Chan et al. (1980) found that distinct large-scale flow patterns surrounding a storm are associated with its turning motion. Chan and Gray (1982) performed a comprehensive study of tropical cyclone motion in the western North Pacific, west Atlantic, and Australian and South Pacific regions that included up to 21 stratifications. Using U. S. Navy Global Band Analysis (GBA) wind fields, Chan (1985) classified western North Pacific Ocean storms according to westward, northward and northeastward motion, and found results that were consistent with previous composite studies based on rawinsonde data. Additional studies, each with different stratifications, have been performed by Neumann (1979), Brand et al. (1981) and Dong and Neumann (1986).

Vertical wind shear has not been previously investigated as a significant synoptic forcing phenomena. This is the objective of the subject study. Composites of vertical shear fields will be based on the total wind fields rather than the fields reconstructed by summing a subset of EOF coefficients as in the previous chapter. Since the composites wind fields derived from the GBA contain flow patterns associated with different storm tracks (Chan, 1985), it is expected that vertical wind-shear fields will also indicate differences in the synoptic forcing on tropical cyclones.

A. PAST-MOTION CATEGORIES

The five past-motion categories used in this study (Fig. 3.1) were proposed by Elsberry and Peak (1986). Table 3 lists the basic features of each category. Categories SLOW and FAST describe the translation speed of the storms within the past 12 h regardless of direction. Categories SO, NW and NE contain storms that moved south, northwest or northeast, respectively, between 2.5 m/s and 8 m/s. Using discriminant

analysis, Elsberry and Peak found that the speed and direction of a storm within the past 12 h could be used as predictors of future tropical cyclone motion. This stratification was also used by Schott (1985), who demonstrated that different synoptic forcing (at single levels) is responsible for whether a storm moves slow, fast, right or left.

Only 1202 of the original 1357 cases are available since 155 cases are missing a past 12-h warning position. The majority of the storms (497) moved northwest at a mean direction of 301°. Schott (1985, his Table 2) summarized the mean and standard deviations of the storms in each category according to speed, direction, intensity and initial latitude and longitude. The storms within Category NW will be further stratified in a later section.

The composite technique is to construct a mean and standard deviation of the zonal and meridional shear values at each of the 527 gridpoints for each of the five past-motion categories. The resultant vertical shear fields also have been normalized to 100 mb for ease of comparison. Differences in the synoptic forcing induced by wind shear then can be studied among the five categories. Composite vector wind shear fields are derived from the square root of the sum of the squares of the individual u and v-shear fields at each level.

Storms in Categories SLOW, FAST, SO, NW and NE will be compared with those in the northwest past-motion category (NW), which is the typical track orientation. Furthermore, this category contains the largest number of cases (Table 3). The composite vector wind shear fields for the deep layer (250-700 mb) for Categories NW and NE are shown in Figs. 3.2a and 3.2b. The 250-700 mb field is selected because this layer incorporates aspects of both the lower- and upper-layer shears. The environment for Category NW storms consists of westerly shear over the entire northern half of the domain. In comparing the fields, it is apparent that storms moving northeast (Category NE) have a much larger directional deviation in the environmental shear than those moving northwest (Category NW). Generally, stronger westerly shear (baroclinicity) is found to the west-northwest and directly north of the storm, as expected for recurving storms. Stronger easterly shear appears to the south in Category NW storms. The thermal ridge line separating westerly/easterly shear regions to the west of the storms is farther north for the Category NW storms. Thus, the northwest motion of these storms is enhanced by the warmer region of air.

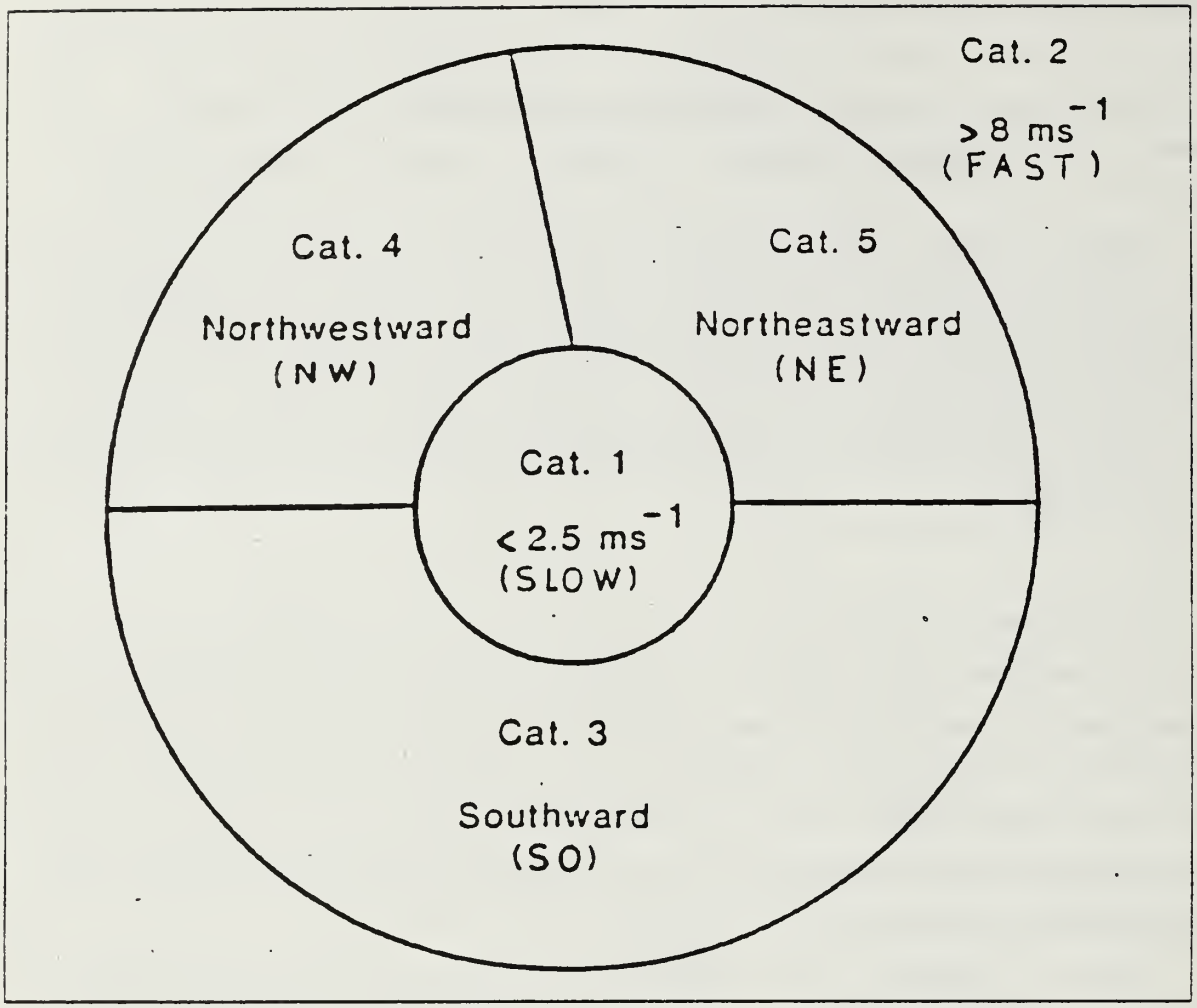

Figure 3.1. Schematic of the five past-motion categories based on the prior 12-h speed and direction classification by Elsberry and Peak (1986).

TABLE 3

Characteristics and sample sizes for the five past-motion categories based on past 12-h motion of the storm.

Category	Characteristic	Sample Size
SLOW	<2.5 m/s	169
FAST	>8.0 m/s	174
SO	091-270°	124
NW	271-340°	497
NE	341-090°	237
Total		1202

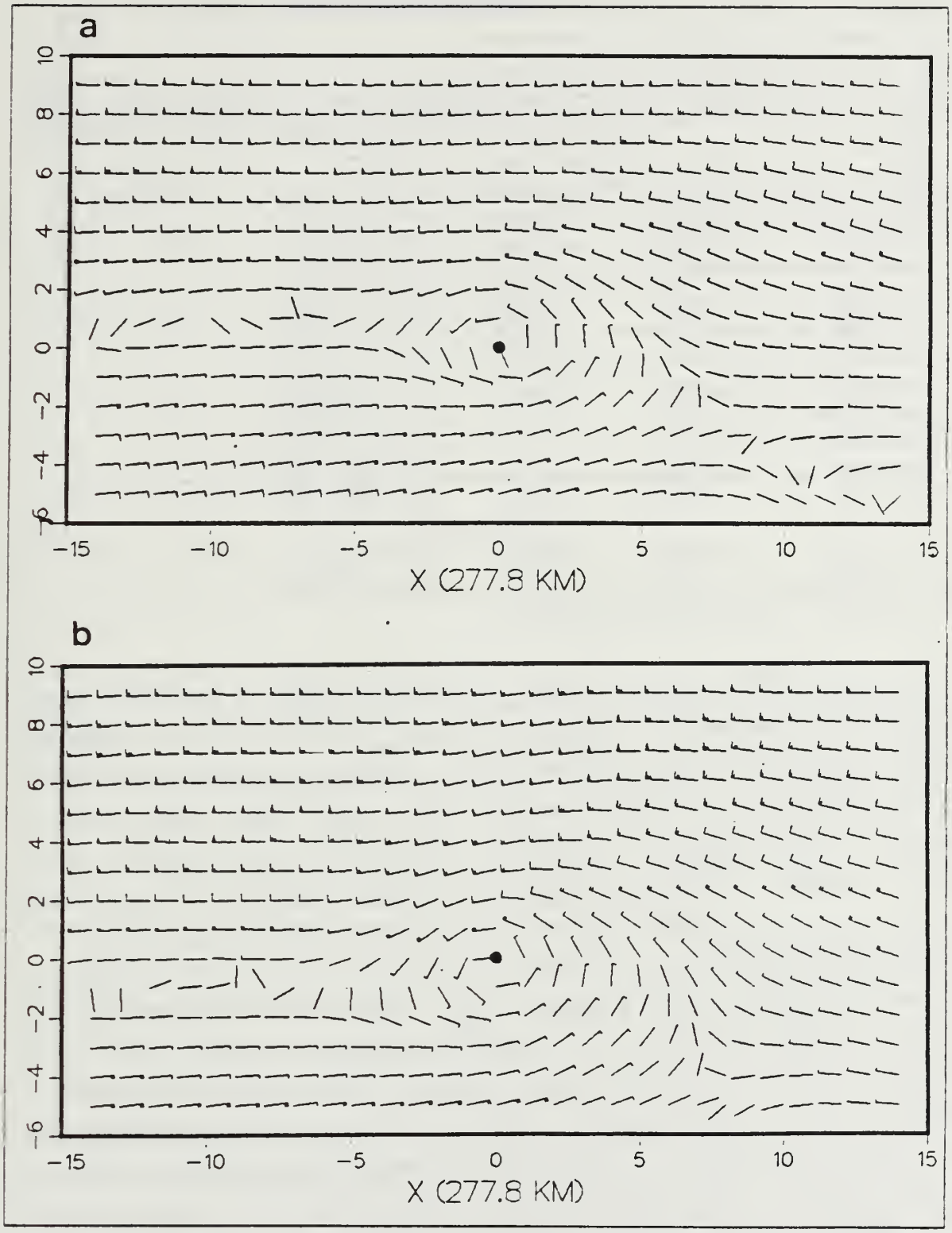

Figure 3.2 Composite 250-700 mb wind shear (m/s per 100 mb) fields for (a) Category NW and (b) Category NE storms. Short (long) windbarbs and flags represent 1 (2.5) and 5 m/s shears.

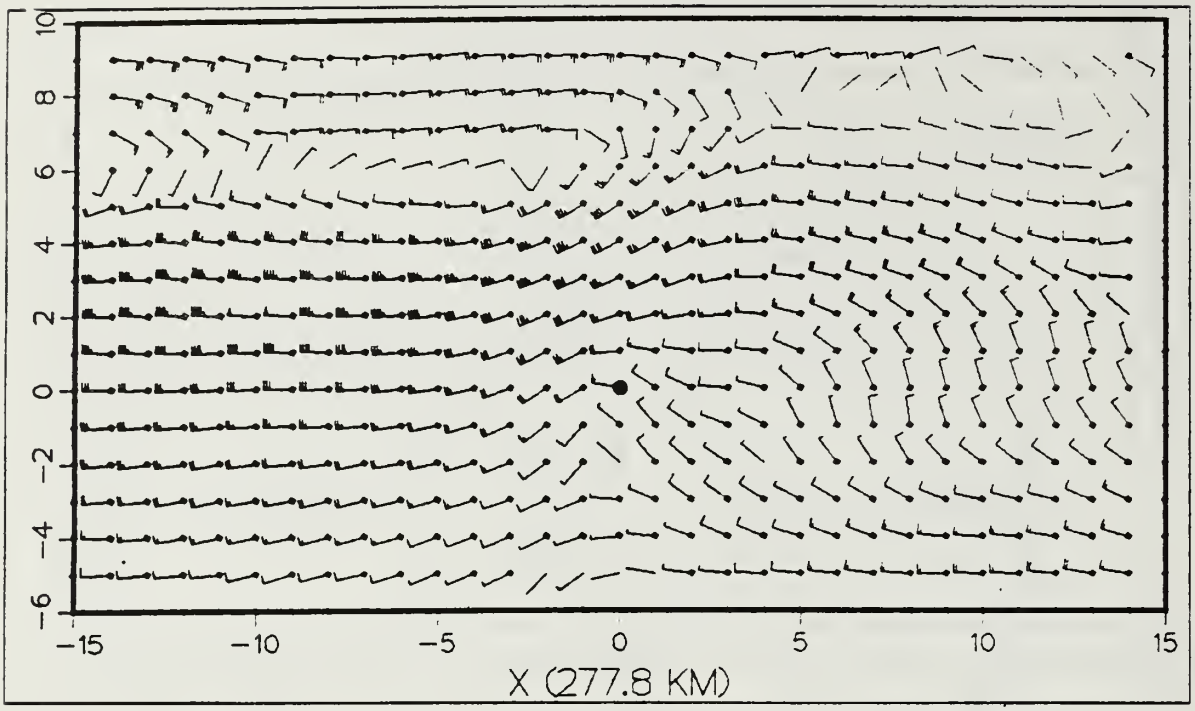

Figure 3.3 Difference in the 250-700 mb wind shear (m/s per 100 mb) for Category NE minus Category NW with symbols as in Fig. 3.2.

Subtracting these composite vector wind fields in Fig. 3.2 emphasizes the differences in the shear features. Subtracting Category NW from the other categories is akin to removing the typical storm environment, with positive (negative) deviations at a gridpoint indicating more positive (negative) shears. The Student's t-test is used to determine if either the zonal or meridional components at each gridpoint are significantly different. The null hypothesis is that there is no difference. For a 95 % confidence of statistical difference, the t-value at a gridpoint must be greater than 1.96. If this occurs for either the u or v component, the total wind vector at that gridpoint is considered to be different. Table 4 lists the number of significant points between each of the five categories for the u, v and vector fields between the various levels. For example, 466 of the 527 gridpoints between Categories NE and NW are statistically different at the 95 % confidence level. Thus 87 % of the gridpoints are different, which is strong evidence that the overall synoptic forcing between these storm-motion categories is different. The difference in shear vectors for Category NE minus NW (Fig. 3.3) illustrates the shear forcing present for northeast-moving storms relative to those moving to the northwest. The basic pattern is for more westerly shear in the

TABLE 4

The number of gridpoints with statistically different u, v and vector shear values within each shear layer and between the categories based on the Student's t-test using a 95 % confidence level statistical difference.

Categories	Shear Layer	U-field	V-field	Vector-field
SLOW - NW	400-700 mb	94	134	206
	250-400 mb	27	171	191
	250-700 mb	61	179	210
FAST - NW	400-700 mb	345	162	406
	250-400 mb	301	168	366
	250-700 mb	356	226	431
SO - NW	400-700 mb	308	183	370
	250-400 mb	197	294	380
	250-700 mb	310	289	425
NE - NW	400-700 mb	439	143	450
	250-400 mb	349	200	427
	250-700 mb	428	197	466
FAST - SLOW	400-700 mb	265	201	373
	250-400 mb	270	156	345
	250-700 mb	311	205	395

Category NE storm relative to that in Category NW storms, especially west of the storm center. This is consistent with more eastward track components in Category NE relative to Category NW. Northerly shear is clearly present to the east of the storm center. A weak (cold) thermal trough is found to the northwest of the tropical cyclone in all three shear layers. Viewed with respect to Category NW, the Category NE storms are colder over and to the north of the tropical cyclone, which corresponds geostrophically to increasingly westerly winds aloft in Fig. 3.3.

Storms that are moving to the south in Category SO (Fig. 3.4), have stronger westerly shear to the north (7 m/s per 100 mb) compared to those moving to the northwest (Category NW). Notice a regular pattern of anticyclonic shear is over and directly to the west of the cyclone. Thus, these cases that have an unusual southward motion appear to be still located in the warm tropical air. The number of gridpoints with significantly different mean shear values between these storm categories is not as great as between Categories NW and NE (Table 4). There are 425 significantly different points in the 250-700 mb layer with an approximate balance between the number of differing u and v components. The largest Category SO minus NW shear differences are to the north of the tropical cyclone, which suggests a more intense

westerly trough in that region for the southward moving (Category SO) storms. It is rather surprising that Category SO storms have southeasterly shear to the east and southwesterly shear to the west of the cyclone center (Fig. 3.5). The forcing that results in these storms moving to the south is not clearly evident, although the region with minimal shear differences (warm ridge) immediately to the west of the storm center may have some role in distinguishing storm motion differences. A warm ridge also appears to east of the storm.

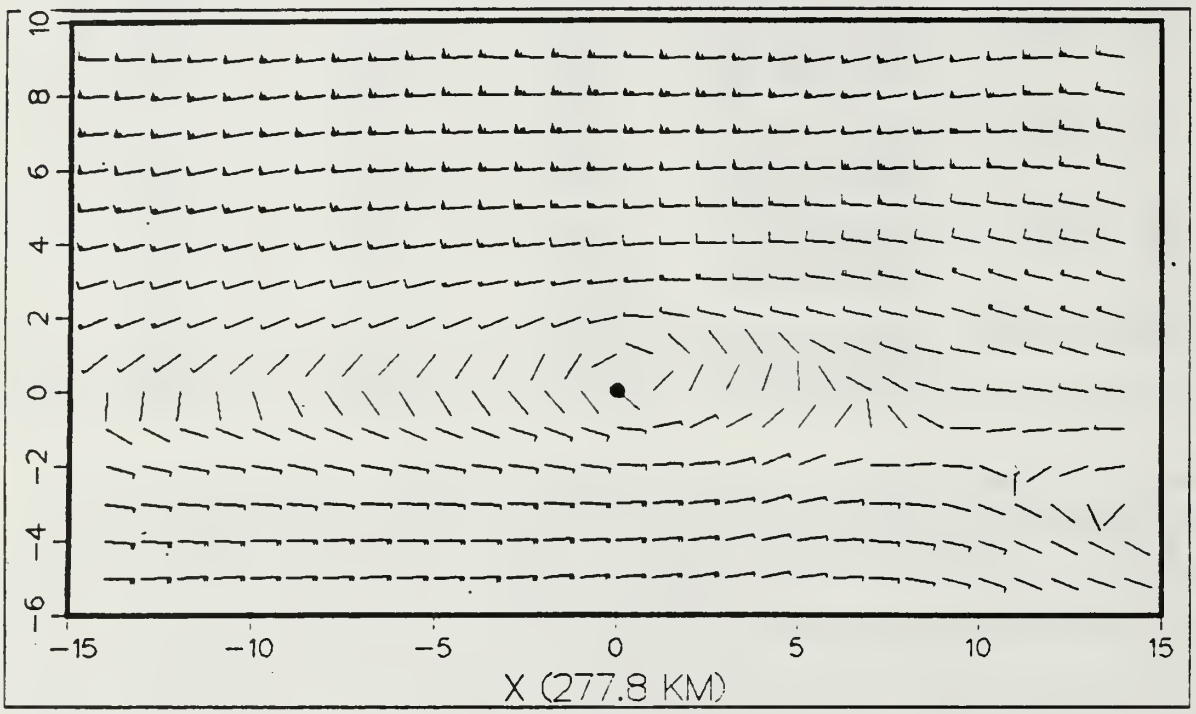

Figure 3.4 As in Fig. 3.2, except for Category SO storms.

There appear to be several similarities between slow storms (Category SLOW) and northwest-moving storms (Category NW). Fast storms (Category FAST) and northeast-moving storms (Category NE) also seem to be similar in pattern. Thus, the differences between slow and fast storms are similar to the Category NE minus Category NW results. The obvious difference between fast-moving (Category FAST) and slow-moving (Category SLOW) storms (Fig. 3.6) is a larger areal extent to their influence of the environment, as is the case for the northeast-moving (Category NE) cyclones. As recurvature occurs and the cyclone enters the region of prevailing westerlies, the storms generally undergo an increase in speed. Thus, some of the fast-

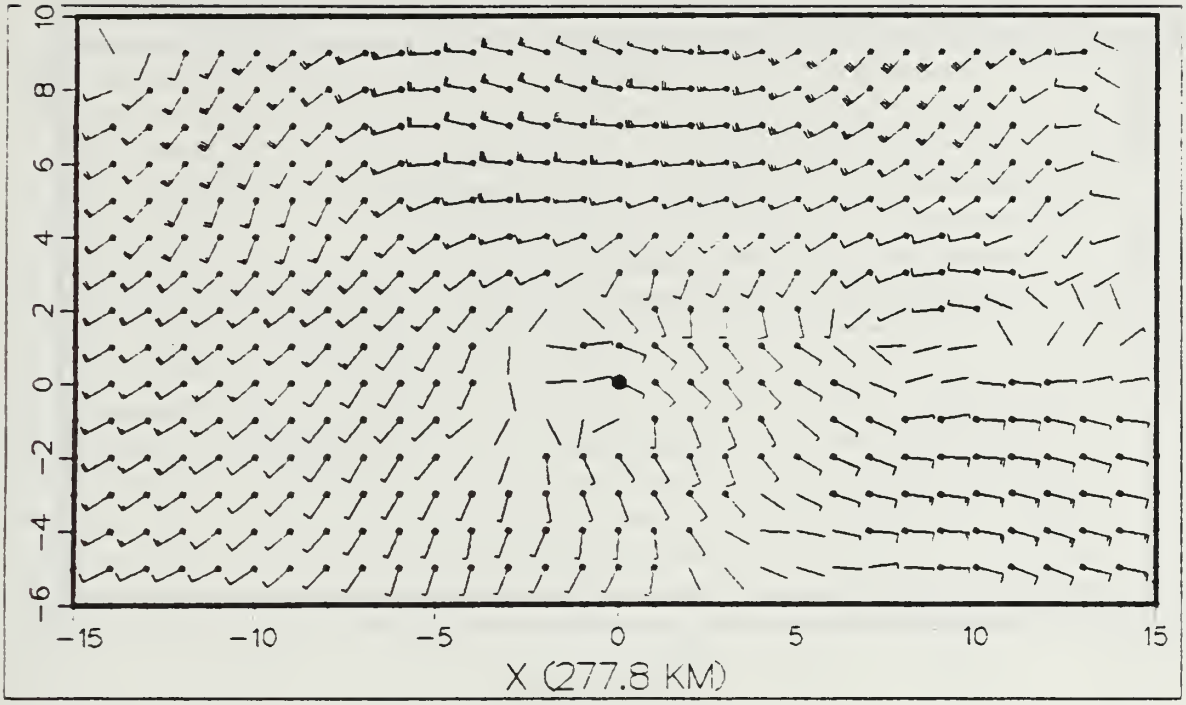

Figure 3.5 As in Fig. 3.3, except for Category SO minus Category NW storms.

moving storms are probably recurvers, which would fit into the Category NE directional stratification. These patterns are not exactly the same because Categories SLOW and FAST contain storms that move in any direction at slow and fast translation speeds, respectively. The number of significant points between Categories SLOW and NW, and between FAST and NE, is less than between Categories SO and NW and between NE and NW, which indicates less statistical difference exists between the former categories. The slower storms have larger westerly shear to the north and northwest, and larger easterly shear to the south than the fast storms (Fig. 3.6). The wind vector difference (Fig. 3.7) shows a thermal (cold) trough to the northwest and far to the northeast for fast relative to slow storms. The strong northeasterly shear just to the west of the cyclone may account for more rapid translation speeds in Category FAST relative to Category SLOW storms.

Low-level shear differences between the categories in Table 4 generally have a greater number of significantly different points than the upper-layer shear fields. Whereas the number of U-shear differences between Categories NW and NE and between Categories SLOW and FAST are larger than the number of V-shear

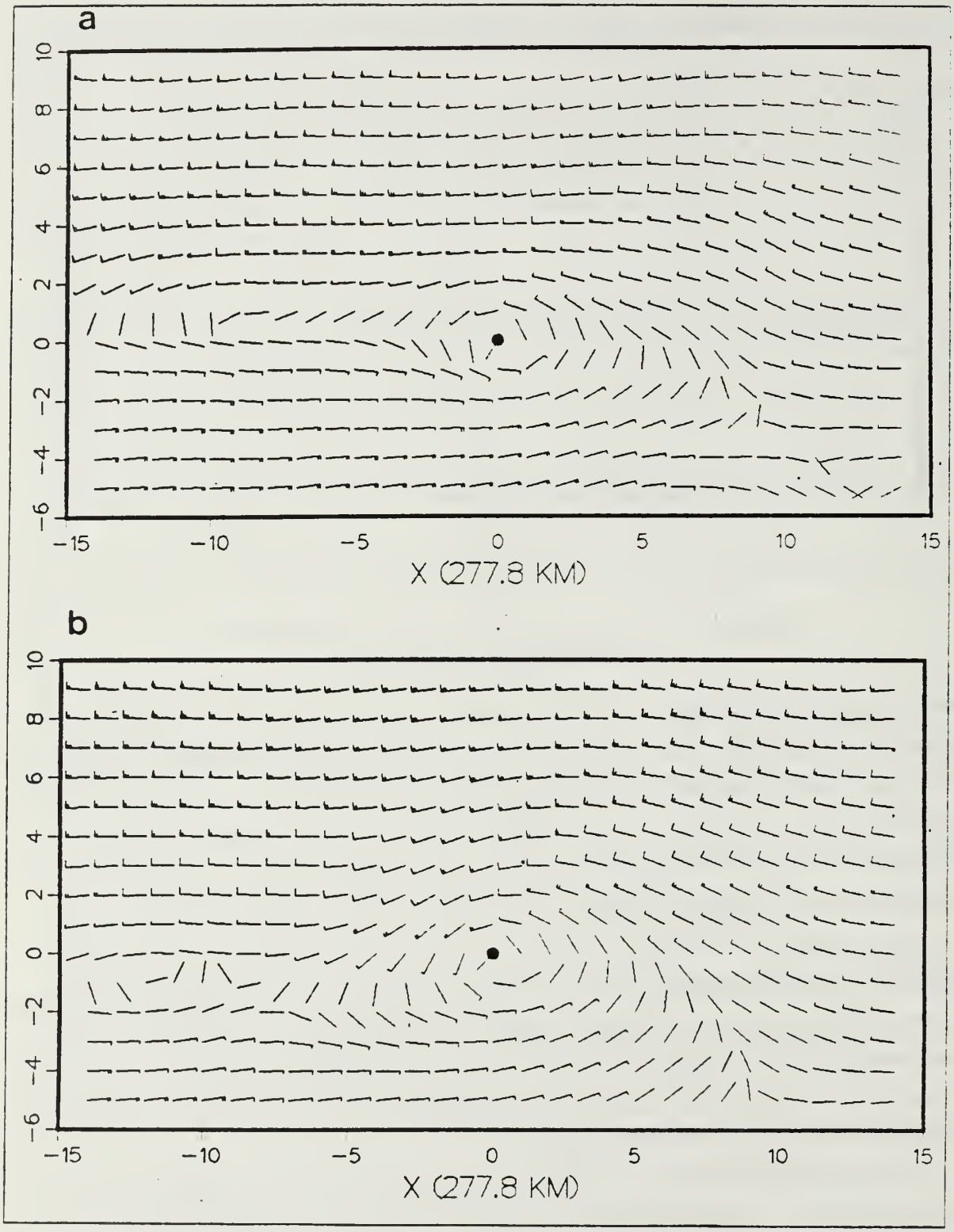

Figure 3.6 As in Fig. 3.2, except for (a) Category SLOW and (b) Category FAST storms.

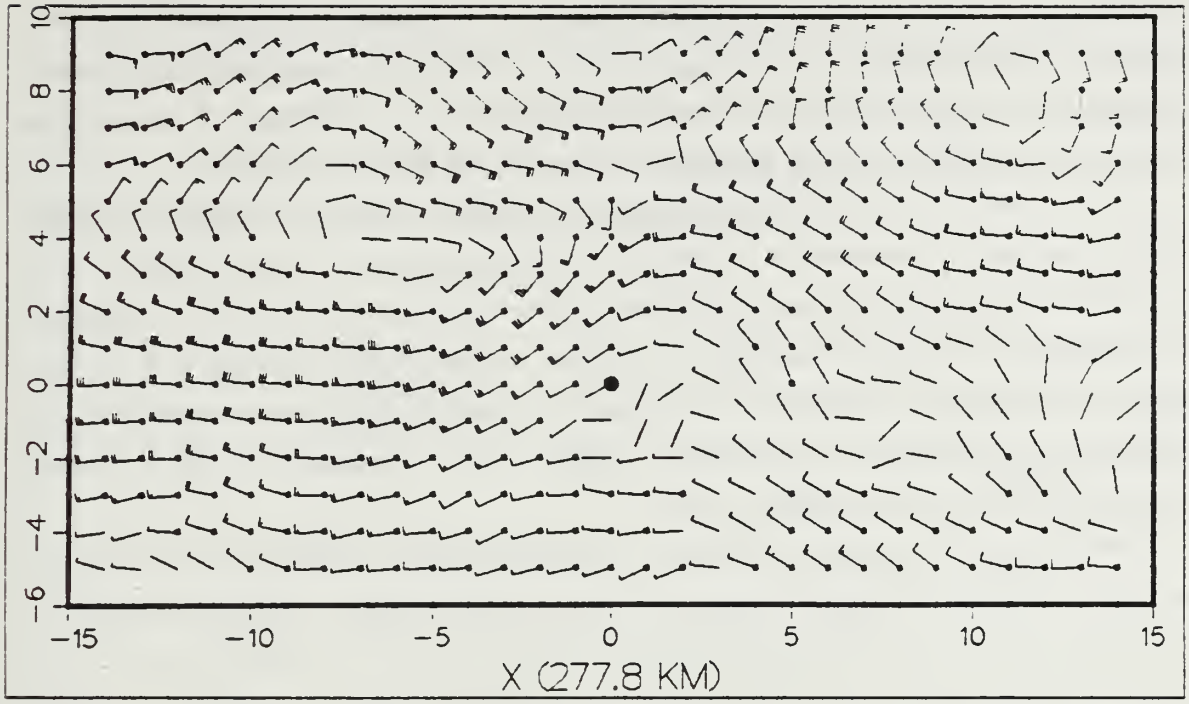

Figure 3.7 As in Fig. 3.3, except for Category FAST minus Category SLOW.

differences in all three layers, the V-shear differences are larger between Categories NW and SO.

B. CATEGORY NW TERCILE COMPOSITE PATTERNS

Neumann and Pelissier (1981) introduced the concept of measuring track error in terms of cross-track (CT) and along-track (AT) displacements relative to the best track orientation at the time of the forecast. Elsberry and Peak (1986) defined the CT/AT components based on the past 12-h warning positions of the cyclone, which effectively normalizes the forecasts relative to a persistence forecast. Warning positions were used, because best track information is not available at the forecast time. In this study, these CT/AT components are referenced to the western North Pacific area version of the CLImatology and PERsistence (CLIPER) forecast of Xu and Neumann (1985). This scheme does not incorporate any dynamic or synoptic forcing and is considered a no-skill forecast. CT/AT components are computed every 24 h relative to the CLIPER forecast track to remove the contributions of persistence and climatology to the 24-, 48- and 72-h forecasts. The CT component refers to the turning motion of the storm relative to a CLIPER forecast. Similarly, the AT component is a measure of

the storm speed relative to the CLIPER track. A positive (negative) CT or AT component indicates motion to the right (left) or fast (slow), respectively. However, any directional change (CT) in the storm motion results in a non-zero AT component even if the actual displacements are equal (Neumann and Pelissier, 1981).

Each storm in a past-motion category is placed into one of three intervals (terciles) regarding its cross-track or along-track motion relative to the CLIPER track. For example, the 72-h positions are chosen to evenly divide the northwest (Category NW) storms into left, center and right CT terciles, or slow, center and fast AT terciles. Based on the sample of storms in each tercile, a mean composite vector wind field is constructed as described in the previous section. For a summary of the statistical properties of each tercile, see Schott (1985).

Table 5 lists the number of points for which significant differences are found in the composite mean U-shear, V-shear and vector shear fields. A Student's t-test is again applied to determine the statistical significance at the 95 % confidence level. The largest shear differences occur between the left and right terciles, as expected. For the cross-track terciles, the largest number of significant points occurs in the U-shear fields in the lower layer. By contrast, there are relatively few points with statistically different meridional shear components between the fields. This implies that the lower-layer shear, especially in the zonal components, is responsible for forcing cross-track motion relative to the CLIPER track.

The differences between left and right terciles within Category NW for the 250-700 mb wind shear are shown in Fig. 3.8. The left CT wind shear field has larger westerly shear to the north, while the right tercile field indicates a weak trough to the northwest of the storm center. The 400-700 mb right minus left composite wind difference field (Fig. 3.9) shows comparatively weak northerly shear dominating the regions to the south and west of the storm. Based on the geostrophic thermal wind, the right-turning storms within Category NW have a weak (cold) thermal trough to the northwest. A study of Table 5 shows little difference in the upper- and deep-layer center minus right, and center minus left, CT terciles.

Generally fewer significant points are found between the AT (speed) terciles. (Table 5). Very few points with significant differences exist between the slow minus center and center minus fast AT terciles. More significantly different shears occur in the lower layers than in the upper layers. However, this occurs to a much lesser extent than for the CT comparisons, in which the lower-layer shear fields are very dominant.

Less than half of the points are statistically different between the fast minus slow tercile in the deep layer. Fig. 3.10 is a plot of the differences between these composite wind fields. In addition to the stronger shear from east-to-west for the fast storms relative to slow storms, there is a southward (rather than the expected northward) shear to the northwest of these Category NW storms.

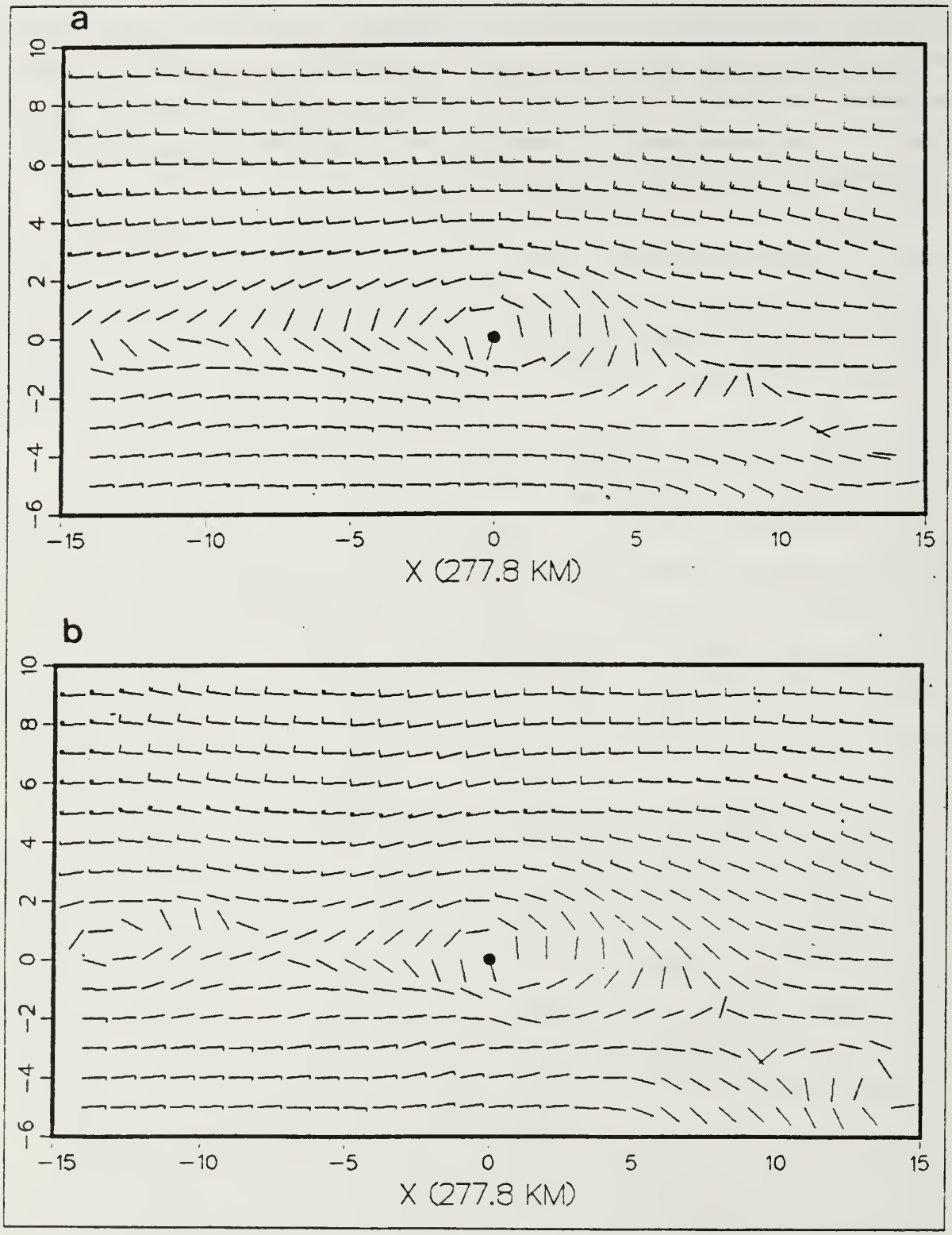

Figure 3.8. As in Fig. 3.2, except for the 400-700 mb shears in the composite (a) left and (b) right terciles of Category NW storms.

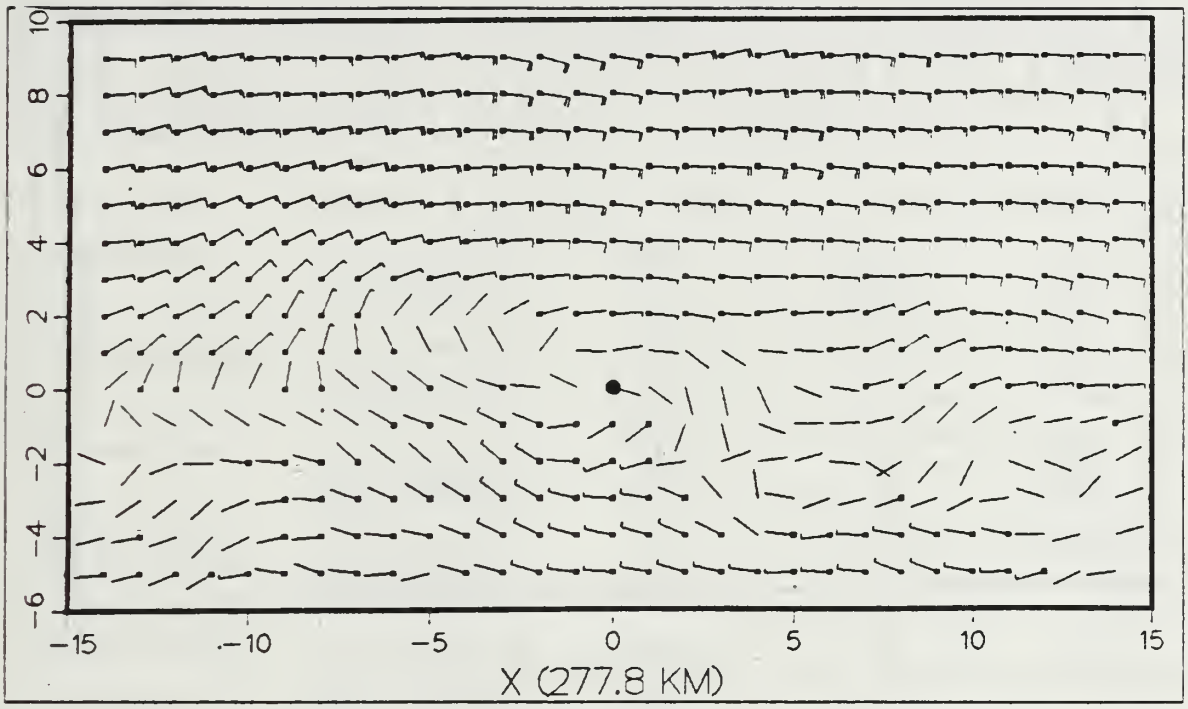

Figure 3.9 As in Fig. 3.3, except for shear differences in the 400-700 mb layer between the right minus left terciles of Category NW storms.

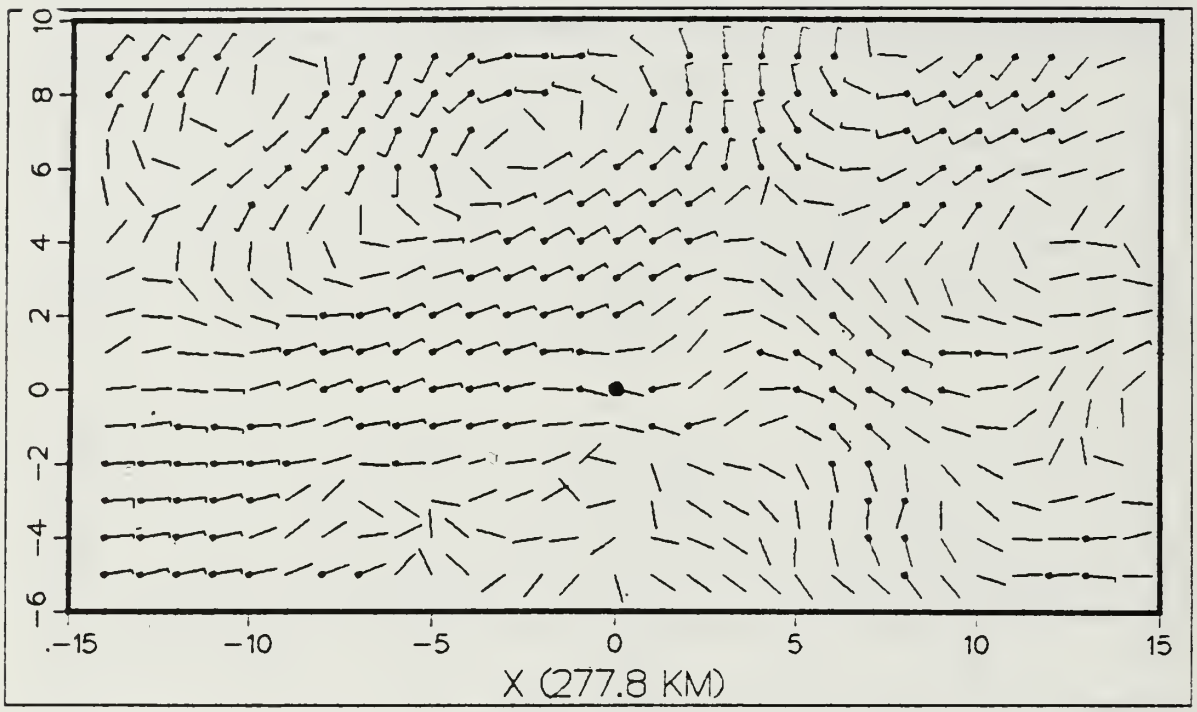

Figure 3.10 As in Fig. 3.9, except for fast minus slow terciles of Category NW storms.

TABLE 5

The number of Category NW gridpoints with statistically different cross-track (right, center and left) and along-track (slow, center and fast) values in the shear levels indicated. Numbers of the U-component, V-component and vector differences indicated separately. Significant difference is based on the Student's t-test using 95 % confidence level.

Tercile	Shear Layer	U-field	V-field	Vector-field
Right-Left	400-700 mb	403	58	421
	250-400 mb	99	123	217
	250-700 mb	110	128	230
Center-Right	400-700 mb	385	13	390
	250-400 mb	21	16	39
	250-700 mb	32	14	36
Center-Left	400-700 mb	119	26	142
	250-400 mb	57	63	117
	250-700 mb	73	70	139
Slow-Center	400-700 mb	91	40	114
	250-400 mb	72	22	89
	250-700 mb	63	38	89
Center-Fast	400-700 mb	22	84	102
	250-400 mb	35	56	87
	250-700 mb	10	72	82
Fast-Slow	400-700 mb	124	129	210
	250-400 mb	89	69	151
	250-700 mb	122	104	204

IV. REGRESSION ANALYSIS

The JTWC employs a variety of objective aids to forecast the motion of tropical cyclones. There are eleven aids available to the forecaster at a tropical cyclone warning time, but no single aid has proven to be effective under all circumstances. Jarrell et al. (1978) has shown that from 1966-1975 forecasting errors decreased to some extent at 72 h while little improvement was seen at 24 h. The gain was due to improvements in objective guidance and availability of satellite images, but this has been partially offset by a reduction of ship reports and aircraft reconnaissance.

A study of objective aids by Tsui (1984) has shown that the One-way Tropical Cyclone Model (OTCM) is better at speed and timing forecasts than the official JTWC forecast but is less accurate in track errors. Elsberry and Peak (1986) found the OTCM was the most skillful at 72 h of the nine objective aids studied in terms of cross-track and along-track components. A similar study by Jones (1986) of four western North Pacific area forecasting aids found the OTCM to be the best overall objective aid, especially for mid- and long-range forecasts. The OTCM forecast error for the sample of storms during 1982-1983 was decreased by over 210 km at 72 h in a post-processing technique developed by Schott (1985). Some of the key predictors in the statistical equations for adjusting the OTCM tracks were the EOF coefficients representing the synoptic forcing at each level. One of the objectives of this work is to determine the predictive skill of the EOF coefficients representing the vertical wind-shear fields. The UCLA Biomedical computer program (BMDP2R) is used to generate the predictors for the regression model to improve the OTCM forecast errors (Dixon and Brown, 1981).

The same set of OTCM forecasts is used in this regression analysis as was used by Schott (1985). The OTCM uses the 12-h old prediction fields to initialize the model for the 00 and 12 GMT forecasts. Currently, the OTCM uses the 00 and 12 GMT analyzed GBA wind fields to initialize the 06 and 18 GMT forecasts, respectively. Although the wind fields used in computing the EOF coefficients for this study encompassed cases from 1979 to 1983, the 06 and 18 GMT OTCM forecasts were not archived from 1979 to 1981 and therefore are not available for use in developing the regression analysis scheme. Thus, the sample selected for testing is drawn entirely from

1982 and 1983 OTCM forecasts, which limits the sample size for 24-, 48- and 72-h forecasts to 267, 212 and 161 cases, respectively. The wind-shear coefficients are added as predictors for this set.

A. POTENTIAL PREDICTORS

As studied by Wilson (1984) and Schott (1985), potential predictors for use in the regression equations include the following five factors on storm motion: (1) Julian date; (2) initial warning position; (3) storm intensity; (4) past storm motion; and (5) external physical forcing represented by the EOF coefficients. The analysis provided potential predictors for the 24, 48 and 72 h forecasts for post-processing the cross-track (CTP) and along-track (ATP) corrections to the OTCM forecast track, where the CTP and ATP components are defined as the OTCM CT/AT components minus the best-track CT/AT components. Hence, the CTP and ATP components adjust the OTCM forecast positions to coincide with the observed position of the tropical cyclone. Wilson (1984) had used a total of 83 predictors which included wind-based EOF coefficients. Schott (1985) added additional wind-based EOF coefficients as predictors for a total of 187 potential predictors. Since there is a maximum of 161 cases at 72 h, this number of predictors is considered excessive. After adding the wind-shear EOF coefficients derived in Chapter II, the total number of potential predictors is 337 (see Table 6). However, a screening process (to be described later) reduces the predictors to only 99 that will be used to derive the equations.

The first four potential predictors (1-4) are derived from observations of the tropical cyclone at the base time. These are the Julian date, JTWC warning latitude and longitude, and maximum sustained wind (intensity). Since relatively few storms have anomalous tracks, persistence of motion has always provided a sound basis for short-term forecasting. The next nine predictors (5-13) describe the storm motion within the past 24 h by means of the zonal and meridional velocity and total vector displacement.

The external synoptic forcing on the tropical cyclone is included as the wind-based EOF coefficients generated by Schott (1985). These represent the environmental wind fields at 700, 400 and 250 mb. Although 35 zonal and meridional modes were found to contain signal, only the first 25 modes at each level are included as potential predictors (14-163). These predictors are identified in the form Clwnn, where C stands for coefficient; l is the level (7 for 700, 4 for 400, and 2 for 250); w stands for the u or v wind component; and nn is the coefficient number from 1-25.

TABLE 6

Potential predictors provided for the regression analysis

Predictor Number	Name	Description
1	JULDATE	Julian date
2	LAT	Warning position latitude
3	LONG	Warning position longitude
4	SPD	Maximum sustained wind speed (kt)
5	VX0012	Zonal cyclone speed from 00 to -12 h (km/h)
6	VY0012	Meridional cyclone speed from 00 to -12 h (km/h)
7	V0012	Total cyclone movement from 00 to -12 h (km)
8	VX1224	Zonal cyclone speed from 12 to -24 h (km/h)
9	VY1224	Meridional cyclone speed from 12 to -24 h (km/h)
10	V1224	Total cyclone movement from 12 to -24 h (km)
11	VX0024	Zonal cyclone speed from 00 to -24 h (km/h)
12	VY0024	Meridional cyclone speed from 00 to -24 h (km/h)
13	V0024	Total cyclone movement from 00 to -24 h (km)
14-38	C7U1-25	700 mb coefficients derived for zonal modes 1 to 25
39-63	C7V1-25	700 mb coefficients derived for meridional modes 1 to 25
64-88	C4U1-25	400 mb coefficients derived for zonal modes 1 to 25
89-113	C4V1-25	400 mb coefficients derived for meridional modes 1 to 25
114-138	C2U1-25	250 mb coefficients derived for zonal modes 1 to 25
139-163	C2V1-25	250 mb coefficients derived for meridional modes 1 to 25
164-166	E12 EY12 EX12	Dist. from 12-h backward extrapolation pt. to -12 h warning position. Meridional and Zonal dist. included
167-169	E24 EY24 EX24	Dist. from 24-h backward extrapolation pt. to -24 h warning position. Meridional and Zonal dist. included
170-172	D2400 DY2400 DX2400	Dist. from 24-h OTCM position to 00 h warning position. Meridional and zonal distances included
173-175	D4800 DY4800 DX4800	Dist. from 48-h OTCM position to 00 h warning position. Meridional and zonal distances included
176-178	D4824 DY4824 DX4824	Dist. from 48-h OTCM position to 24 h warning position. Meridional and zonal distances included
179-181	D7200 DY7200 DX7200	Dist. from 72-h OTCM position to 00 h warning position. Meridional and zonal distances included
182-184	D7248 DY7248 DX7248	Dist. from 72-h OTCM position to 48 h warning position. Meridional and zonal distances included
185-187	D7224 DY7224 DX7224	Dist. from 72-h OTCM position to 24 h warning position. Meridional and zonal distances included

TABLE 6

(cont'd.)

188-212	S47U1-25	400 minus 700 mb shear coefficients derived for zonal modes 1 to 25
213-237	S47V1-25	400 minus 700 mb shear coefficients derived for meridional modes 1 to 25
238-262	S27U1-25	250 minus 700 mb shear coefficients derived for zonal modes 1 to 25
263-287	S27V1-25	250 minus 700 mb shear coefficients derived for meridional modes 1 to 25
288-312	S24U1-25	250 minus 400 mb shear coefficients derived for zonal modes 1 to 25
313-337	S24V1-25	250 minus 400 mb shear coefficients derived for meridional modes 1 to 25

The next set of predictors describes the backward extrapolation and forward forecast track from the OTCM (Fig. 4.1). Predictors 164-169 describe the total, meridional and zonal distances that the OTCM +24 h OTCM position would be displaced if extrapolated backward through the 00 h storm position to a -24 h position. This backward extrapolation method was developed by Peak and Elsberry (1982) to include any initial track orientation error as a predictor. For example, the predictor E24 is the adjustment to the +24 OTCM forecast position that would be necessary to rotate the OTCM forecast track along the persistence track over the past 24 h. The -12 h position (E12) is extrapolated from a position one half the distance to the +24 h position since the +12 h position is not available. Predictors 170 to 187 describe combinations of the forward 24-, 48- and 72-h distances to account for variations in the forecast track orientations. This can be used to give insight into the CTP components that are necessary during recurvature. For example, DY7200 describes the meridional distance the storm has travelled from the 00 warning position to the 72-h OTCM position (Fig. 4.1).

The remaining predictors (188-337) are the wind-shear EOF coefficients generated in Chapter II. These represent the synoptic forcing upon storm motion by differences in the wind through three vertical layers in the storm environment. These potential predictors are identified as Sllwnn, where S stands for wind shear; ll stands for the layer (47 for 400 minus 700 mb, 27 for 250 minus 700 mb, and 24 for 250 minus 400 mb); w is the u or v component; and nn is the coefficient number from 1 to 25.

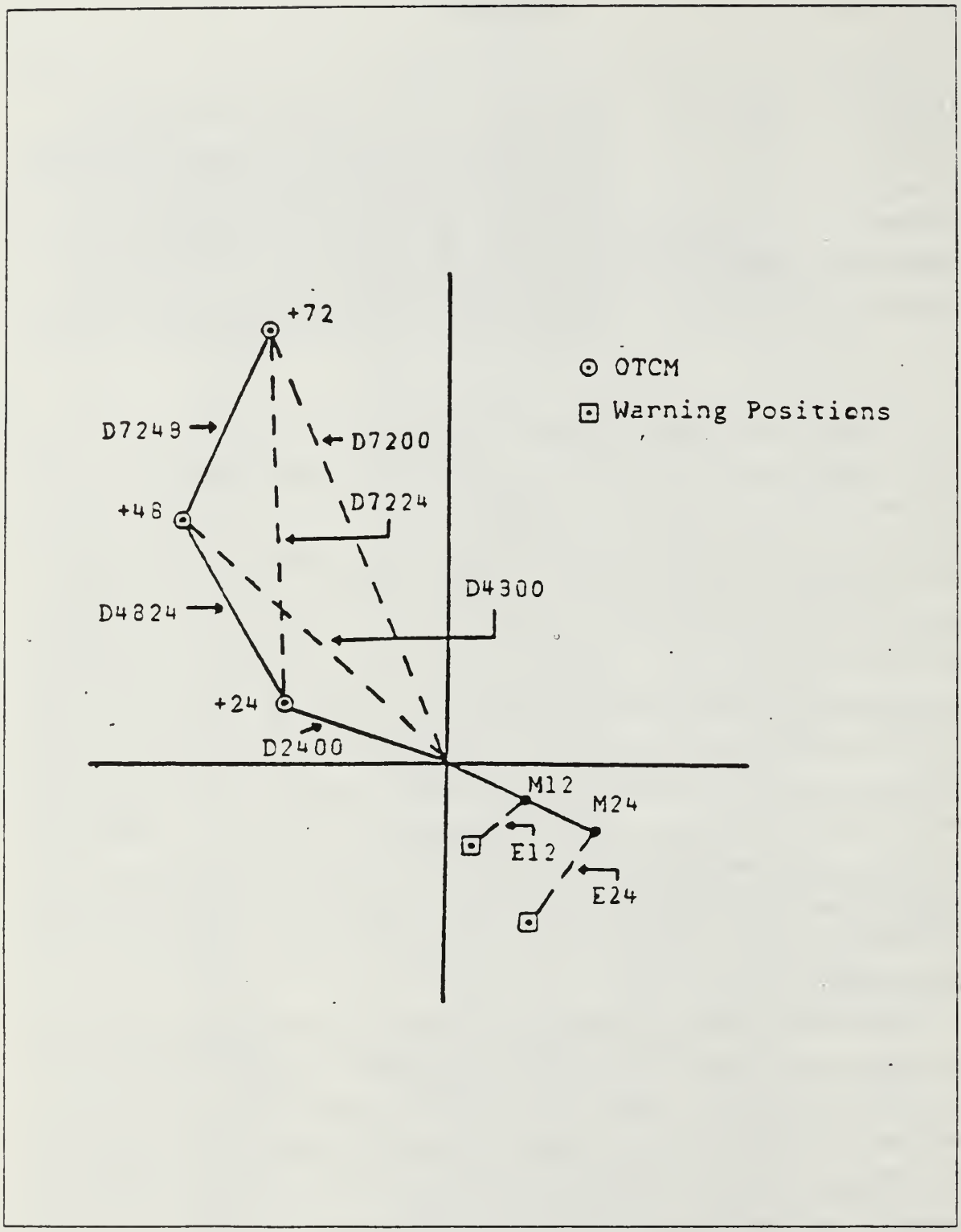

Figure 4.1 The OTCM forecast positions at +24, +48 and +72 h (circled dots) and backward extrapolation positions at M12 and M24 h that are used to define potential predictors (Table 6) in the regression analysis.

B. REGRESSION EQUATIONS

To predict the CTP and ATP adjustments to the OTCM forecast track at 24, 48 and 72 h, a stepwise regression analysis is used. Since wind-shear EOF's have been demonstrated to represent synoptic forcing on tropical cyclone motion in Chapter III, the EOF coefficients can be used to explain a portion of the variance in CT and AT components used to adjust the OTCM track. The coefficient of multiple regression (R^2) is a measure of the relationship between independent and dependent variables in the regression model and represents the amount of total variance in the predictand that is explained by these variables,

$$R^2 = SSR / SSTO = 1 - (SSE / SSTO), \qquad (4.1)$$

where SSR is the regression sum of the squares, SSTO is the total sum of the squares and SSE is the residual sum of the squares. At each step in the BMDP2R regression analysis routine, that predictor from the remaining set is selected which has the highest partial correlation with the predictand, given the previous selection of predictors. The selection continues until the new predictor does not meet the minimum F-to-enter value of 4.0. In this way, the predictand is the result of a sum of uncorrelated independent variables (Dixon and Brown, 1979). As a further restriction on the number of predictors in the equations, only those predictors that increase R^2 by 0.01 are retained.

Due to the large number of potential predictors available and the limited sample of cases at 72 h, the list of predictors is screened twice to reduce its size. The set of predictors in Table 6 is divided into four categories: (i) persistence predictors; (ii) backward extrapolation and forward track predictors; (iii) wind-based EOF coefficients; and (iv) wind-shear EOF coefficients. Those predictors within each category that remain after a maximum 10-step regression analysis were used to develop regression equations to post-process the OTCM using all but the wind-shear EOF predictors. This was done to compare the results obtained by Schott (1985) against those obtained by this screening method. A total of 96 predictors were found to be important in at least one of the six equations (CTP and ATP at 24, 48 and 72 h). This is far less than the 187 predictors used by Schott. The results (Table 7) show little difference until the 72-h forecast, where an increase of error of over 50 km occurs.

A further screening is accomplished after adding the wind-shear predictors to the set selected by the first screening process. In this screening, only those predictors that occur in more than one of the six regression equations (CT or AT at 24, 48 or 72 h) are selected. Although this process does reduce the explained variance in the regression analysis, we can have confidence in the application of the regression equations to an independent sample.

TABLE 7

Comparison of forecast errors (km) obtained for 24, 48 and 72 h for the unmodified OTCM (OTCM), the modified OTCM results obtained by Schott (1985) using all 187 predictors (OTCM187) and the errors found after a screening process reduced the number of predictors (excluding wind-shear EOF coefficients) to 96 (OTCM96).

	Forecast Errors (km)	
24 h	Mean	Std. Dev.
OTCM	202	121
OTCM187	143	88
OTCM96	144	90
48 h		
OTCM	386	202
OTCM187	286	148
OTCM96	289	152
72 h		
OTCM	593	356
OTCM187	383	256
OTCM96	435	270

Tables 8 and 9 list the equations for the CTP and ATP predictands developed by the regression analyses. A final total of 99 potential predictors were used to generate these equations. Table 10 shows the R^2 values for each equation.

A study of Tables 8 and 9 show that only four wind-shear EOF coefficients that occur more than twice enter the equations compared to 18 wind-based EOF coefficients. This may be due to the close relationships between the wind-based and wind-shear synoptic forcings. After a wind-based predictor is selected, the wind-shear predictors that are highly correlated with it will not be selected. However, the selection of wind-shear predictors does indicate that independent information is contained in these coefficients. However, no wind shear predictors occur in the ATP equations. It is also interesting that there are no deep layer (250 minus 700 mb) EOF predictors

TABLE 8

Regression equation for the CTP adjustments (km) at 24, 48 and 72 h. The number in parenthesis is the order in which the predictors were selected by the regression analysis.

	Forecast Interval (h) 24	48	72
Y-Intercept	11.7	-29.9	-222.0
Predictor			
DayJul	-	-	1.0 (1)
C2V1	-	8.9 (1)	33.3 (2)
C7U7	7.1 (4)	26.1 (3)	48.3 (3)
EY12	0.3 (6)	0.7 (6)	1.0 (4)
D7200	-	-	0.6 (5)
D7224	-	-	-1.1 (6)
C4V13	-	-14.7 (2)	-
C7U21	12.6 (5)	37.3 (4)	-
C7V7	-	12.5 (5)	-
S47U17	-	-26.5 (7)	-
S47V4	3.8 (8)	7.7 (8)	-
S24U18	-	-32.2 (9)	-
C2V17	7.5 (1)	-	-
C4U6	-7.1 (2)	-	-
C4U15	-11.2 (3)	-	-
EX24	0.3 (7)	-	-
S24V12	-6.7 (9)	-	-

chosen in the CTP equations. Of the wind-shear predictors, two low-level and two upper-level coefficients are selected. Table 11 summarizes the number of wind-based and wind-shear EOF predictors chosen by the regression analysis for use in the equations. Only a few (9) predictors occur in more than one equation. Of these, four have an effect on all three forecast times. Among these is the EY12 predictor that enters three times for the CTP equations and twice for the ATP equations. This is not surprising since this predictor is a crucial part of the post-processing scheme of Elsberry and Frill (1980) and Peak and Elsberry (1982). In addition, the latitude is important in all three ATP equations.

C. POST-PROCESSING THE OTCM

To test the validity of this method in adjusting the OTCM forecast to reduce the effect of systematic errors and inadequate representations of synoptic forcing, the CTP and ATP adjustments based on the dependent sample are applied to the OTCM track. The forecast error in the OTCM is defined as the great circle distance between the best-track position of the tropical cyclone and the newly modified OTCM position. Table 12 summarizes the forecast errors between the best-track position and the

TABLE 9

As in Table 8, except for regression equations for ATP (km).

	Forecast Interval (h) 24	48	72
Y-Intercept	176.4	288.7	588.9
Predictor			
XLAT	-12.5 (1)	-23.5 (1)	-43.4 (1)
C2U5	-8.0 (3)	-12.3 (2)	-17.7 (2)
C4V24	-	-26.1 (7)	24.6 (3)
C7U12	-8.3 (5)	-22.5 (4)	50.0 (4)
C7U14	-	-	47.8 (5)
C7V7	-	-	30.3 (6)
EY12	-	-0.9 (8)	-1.0 (7)
E24	-	-0.4 (9)	-0.5 (8)
DX7200	-	-	-1.0 (9)
DX7224	-	-	2.2 (10)
C2V24	-	19.9 (3)	-
C4U15	-	-19.3 (5)	-
C4U16	-11.5 (6)	-28.6 (6)	-
DX4824	-	0.8 (10)	-
VY1224	4.3 (2)	-	-
C2V24	12.4 (4)	-	-
C7V7	-9.6 (7)	-	-
E12	-0.5 (8)	-	-

TABLE 10

Percentage of the explained variance (R^2) in the regression equations for the CTP and ATP predictands.

Time	Number of Cases	Number of Predictors	R^2 CTP	R^2 ATP
24	267	CTP 9	0.392	-
		ATP 8	-	0.392
48	212	CTP 9	0.450	-
		ATP 10	-	0.474
72	161	CTP 6	0.418	-
		ATP 10	-	0.520

unmodified OTCM, the OTCM modified by the regression model and the official JTWC forecast positions for 24, 48 and 72 h.

As indicated above, Schott used 187 potential predictors to derive 72-h regression equations that contained only 161 cases. As a result, his 383 km forecast error at 72 h (compared to 631 km for JTWC) based on the dependent sample may be overly optimistic. When his set of predictors (excluding the wind-shear EOF predictors) was

TABLE 11

The number of wind-based and wind-shear EOF coefficients chosen by the regression scheme as predictors for CTP or ATP.

Level	Field	CTP 24	CTP 48	CTP 72	ATP 24	ATP 48	ATP 72	Total
700	u	2	2	1	1	1	2	9
	v	0	0	0	0	0	1	1
400	u	2	1	0	2	3	0	8
	v	0	1	0	0	0	1	2
250	u	0	0	0	1	1	1	3
	v	1	1	1	1	1	0	5
	Total	5	5	2	5	6	5	28
400-700	u	0	1	0	0	0	0	1
	v	1	1	0	0	0	0	2
250-700	u	0	0	0	0	0	0	0
	v	0	0	0	0	0	0	0
250-400	u	0	1	0	0	0	0	1
	v	1	0	0	0	0	0	1
	Total	2	3	0	0	0	0	5

screened as outlined above, the error at 72 h increased to 435 km. By including the wind-shear EOF coefficients, this error is reduced to 419 km. This results in a 30 % and 33 % error reduction over the unmodified OTCM and official JTWC forecast errors for this set of dependent storms during 1982-1983. The standard deviations at each forecast time are also significantly improved, which means the modified OTCM forecasts are more consistent than the unmodified OTCM. Thus, use of these equations to modify the OTCM forecast track has proven to be successful.

A caution is necessary at this point. The regression equations have been derived and tested on the same dependent set of cases. The model could have a bias toward storm conditions similar to those during 1982-1983 from which the equations were generated. This model should be tested against an independent data set to determine if the EOF predictors chosen would accurately represent the synoptic forcing on other storms with differing wind-shear environments. The model would not be expected to perform as well when anomalous storms occur.

TABLE 12

Mean and standard deviation of the forecast errors (km) for the unmodified OTCM forecast (OTCM), OTCM forecast modified by the regression equations with 99 predictors (OTCM99), and official JTWC forecast errors for 24, 48 and 72 h.

Time	N	Method	Forecast Errors (km) Mean	Std. Dev.
24	245	OTCM	202	121
	245	JTWC	206	126
	245	OTCM99	147	92
48	200	OTCM	386	202
	190	JTWC	443	284
	200	OTCM99	279	154
72	161	OTCM	593	356
	151	JTWC	631	400
	161	OTCM99	419	261

V. DECISION TREE APPROACH

Another concern of the JTWC forecaster is selecting which objective aid will give the most accurate 72-h forecast. If the optimum objective aid could be selected in each storm case, there would be a significant reduction in the mean forecast errors (Tsui, 1984). For example, the mean forecast error at 72 h would be reduced by 56 %. A classification tree algorithm developed by Breiman et al. (1984) has been adapted by Peak and Elsberry (1987) to isolate the significant factors affecting the performance of each aid. A feasibility study of this approach to select the best of three analog forecasts at 72 h was conducted by Peak and Elsberry (1985). The subsequent study by Peak and Elsberry (1987) included predictors such as the wind EOF coefficients and found that the tree selected the best aid from a set of eight aids in 44 % of the cases in the dependent sample.

The basic assumption is that storm-related parameters, such as cyclone size and intensity, and synoptic forcing factors can be used to determine which aid will perform best in a given situation. A data base of storm cases containing the following parameters is constructed: (1) initial latitude and longitude; (2) zonal, meridional and total displacements from 00 to -12 h, 00 to -24 h, and -12 to -24 h; (3) cyclone intensity (maximum wind speed) and size (radius of 15 m/s winds); (4) intensity change between 00 and -12 h; (5) Julian date; (6) zonal and meridional wind EOF coefficients 1-10; (7) zonal and meridional wind-shear EOF coefficients 1-10; and (8) zonal, meridional and total displacement of the CLIPER forecast track from 00 to +24 h; +24 to +48 h; and +48 to +72 h. The number of synoptic and storm-related parameters available to choose from is very large (Table 6, above). In order to work with a manageable set of parameters, only 10 each of the zonal and meridional EOF coefficients is used. The classification tree algorithm will isolate the most significant factors that characterize the performance of each of the eight objective aids. It is possible that a particular aid may have given the best 72-h forecast by coincidence. If the decision tree is to be successful, the selection of the best aid by the tree must be based on real, physically understandable decisions that can be interpreted by the forecaster.

A. DECISION TREE DESCRIPTION

The classification tree examines a set of measurements and assigns each case to a particular class based on the values of the measured parameters. In particular, a class would include all those cases in which a single objective aid is found to be superior at 72 h based on values of the storm-related and synoptic parameters in those cases. Thus, all cases are repeatedly divided into subsets until similar cases are isolated in the same subset, which is called a terminal node. A more complete description of the decision tree algorithm approach is provided in Peak and Elsberry (1987).

A sample of 325 cases from 1981-1984 is selected for this study. A dependent sample of 217 cases is used to develop the tree and 108 cases are set aside for testing. Each case must have 72-h forecasts from the following objective aids: (1) TYphoon ANalogs (TYAN) for recurving storms (RECR); (2) TYAN analogs from the total analog base (TOTL); (3) climatology forecasts (CLIM); (4) extrapolated tracks from the 00 to -12 h positions (XTRP); (5) average of the CLIM and XTRP tracks (HPAC); (6) climatology and persistence forecasts (CLIP); (7) One-way influence Tropical Cyclone Model (OTCM); and (8) Nested Tropical Cyclone Model (NTCM). The Annual Tropical Cyclone Report (NAVOCEANCOMCEN/JTWC, 1984) contains a description of these objective aids.

The decision tree approach is such that the tree can "learn" from past cases and structure the decision process based on all relevant information. A yes/no decision is made for each node based on a particular measured parameter that splits the case sample into subsets that "travel" down the right or left branches. When the inequality used at each node is true, the progression continues down the left branch. Alternate splitting parameters may be used if the primary set of parameters is missing. Subsequent nodes are split and similar cases are progressively isolated until a terminal node is encountered. The terminal node is assigned the objective aid of the class that occurs most frequently in that node.

The decision tree created from the dependent sample is shown in Fig. 5.1. The synoptic forcing is an extremely important factor to consider in selecting an objective aid. The wind EOF coefficients clearly form the basis for separating the cases into their respective classes. Of the eight splits, seven are based on wind EOF coefficients, and of these, four involve the zonal 700 mb component. The dominance of the low-level wind parameters was also found by Peak and Elsberry (1987), where seven of the 15 splitting nodes were based on the 700 mb EOF coefficients. The only non-synoptic

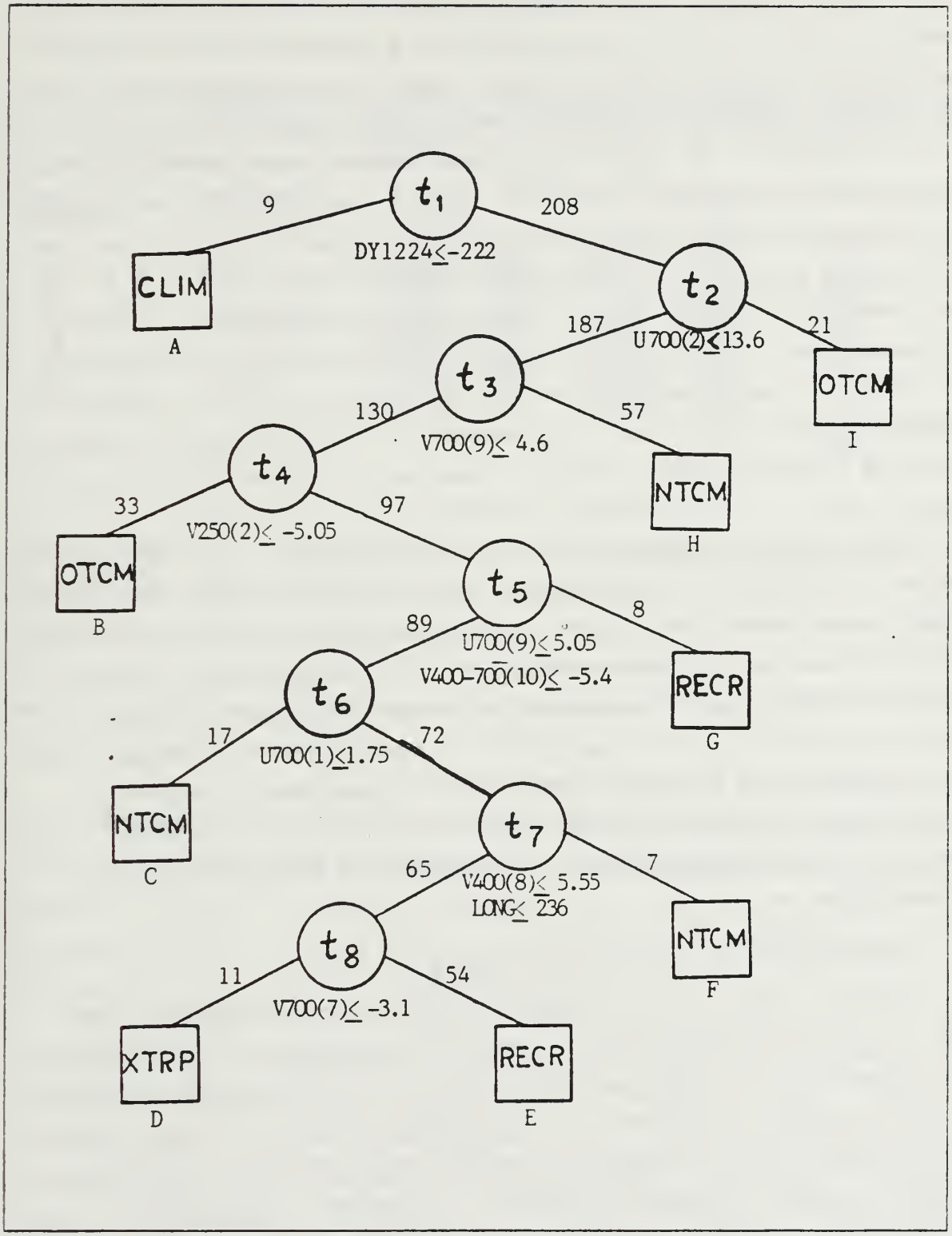

Figure 5.1 Decision tree developed for selecting the objective aid with the minimum 72-h forecast error. Splitting variables and values are listed under each circular node (t_n, n=1,8). Terminal (square) nodes named for aid of the majority of cases in the node. Number of dependent sample cases indicated above each branch.

primary splitting parameter is the meridional persistence component (DY1224) that appears in the first node (t_1). Alternate node-splitting parameters occur at node t_5, in which the 400-700 mb shear of the meridional component appears, and at node t_7, in which the initial storm longitude is used in place of an EOF coefficient.

An objective aid is selected within each terminal node according to the predominant class assignments in each case. Table 13 identifies the first and second most prominent aids found in each terminal node. For example, of the nine cases that fell in terminal node A, CLIM was the most accurate forecast model at 72 h (four cases) followed by TOTL (two cases). Therefore, CLIM is assigned the class name to that terminal node. In practice the forecaster would select the CLIM forecast aid for every storm with parameters that lead to that terminal node. The number of assignments per class range from 57 (terminal node H) to seven (in terminal node F). The NTCM is the most frequently selected forecast aid and is found in three terminal nodes into which 37 % of the dependent sample cases fall. The OTCM is the second most frequently selected terminal node with 24 % of the cases. CLIP, TOTL and HPAC are never chosen for terminal nodes. Thus, the cases for which these models actually provide the best 72-h forecast must be misclassified by the tree. The IND column of Table 13 lists the number of cases from the independent sample that fell into each terminal node. Since the independent sample has half the number of cases, the entries in this column should be roughly 50 % of those in the second column. The largest differences are in the node I, which has only two cases versus an expected 10 or 11, and in node D, which has 10 entries versus the expected 5-6. In the other nodes, the variations from the expected number of assignments can probably be attributed to the small sample size.

B. VERIFICATION OF THE DECISION TREE

A summary of the results of the decision tree for the dependent sample is listed in Table 14. For the dependent sample, the tree selected the correct aid in 27 % of the cases compared to 44 % by Peak and Elsberry (1987). The OTCM provides the lowest 72-h forecast error in the majority of cases (39) followed by the NTCM (37 cases). The OTCM and NTCM are expected to provide better guidance by incorporating dynamical processes in the model. However, it is important to understand when to reject the guidance of these numerical models. This is a main advantage of using the classification tree method. The NTCM has the highest percentage of correct

TABLE 13

First (1) and second (2) most predominant classes of cases in terminal nodes A-I (Fig. 5.1) for the dependent (DEP) and independent (IND) samples. Percentage of cases belonging to each class are in parentheses.

Terminal Node	Number of cases	DEP 1		DEP 2		IND
A	9	CLIM	(44)	TOTL	(22)	6
B	33	OTCM	(30)	CLIP	(18)	21
C	17	NTCM	(52)	CLIM	(17)	12
D	11	XTRP	(63)	RECR	(18)	10
E	54	RECR	(24)	OTCM	(19)	24
F	7	NTCM	(43)	OTCM	(14)	5
G	8	RECR	(50)	OTCM	(25)	1
H	57	NTCM	(24)	XTRP	(19)	27
I	21	OTCM	(31)	XTRP	(19)	2
TOTAL	217					108

classifications (70 %) by the decision tree, and the second highest percentage (58 %) is for the RECR. Cases may be misclassified due to statistical noise, sampling problems, or the pruning process inherent in the decision tree algorithm (Breiman et al., 1984). Of those cases misclassified, the NTCM model was selected 55 times and the OTCM was selected 39 times. Thus, it appears the tree relied on numerical guidance when uncertainty existed in the classification of a case.

A comparison of the overall mean and standard deviation of the 72-h forecast errors (Table 15) shows that if the best aid were selected in each case, a 318 km error would occur. However, Peak and Elsberry (1987) demonstrated that this is not a true measure of the skill of a selection technique because this includes many purely coincidental selections. By using the tree, a 640 km error is achieved compared to the 721 km error for the official JTWC average forecasts.

The independent sample consisted of 108 storm cases. Table 16 lists the classification results from the decision tree for the eight objective aids. The results are disappointing since the tree only classified 19.4 % of the cases correctly. A random selection among the aids would have yielded a 12.5 % correct classification. The misclassifications of TOTL, HPAC and CLIP are expected since these aids do not appear as terminal nodes in the decision tree. However, the scheme does not isolate a significant (more than 12.5 %) number of cases for RECR, CLIM and XTRP in the independent sample. Only the dynamical models continue to be properly selected by

TABLE 14

Decision tree selection of objective aids for the dependent sample cases. The main diagonal contains the number of correct classifications by the tree.

		TRUE CLASS							
		RECR	TOTL	CLIM	XTRP	HPAC	CLIP	OTCM	NTCM
PREDICTED CLASS	RECR	17	2	4	9	7	6	12	5
	TOTL	0	0	0	0	0	0	0	0
	CLIM	1	2	4	0	0	1	1	0
	XTRP	2	1	0	7	0	1	0	0
	HPAC	0	0	0	0	0	0	0	0
	CLIP	0	0	0	0	0	0	0	0
	OTCM	6	5	2	7	5	8	15	6
	NTCM	3	5	7	11	7	11	11	26
	SUM	29	15	17	34	19	27	39	37
% CORRECT		58	0	23	21	0	0	38	70

TABLE 15

Overall mean and standard deviations of the 72-h forecast errors (km) for the dependent sample as selected by the decision tree (TREE), if the BEST and WORST objective aid were always chosen, and the CLIP and JTWC forecasts. The JTWC values are for 193 cases compared to 217 cases for the others.

	TREE	BEST	WORST	CLIP	JTWC
Mean	640	318	1224	703	721
Std. Dev.	484	249	634	480	474

the decision tree. However, the mean forecast error in the independent sample (Table 17) of 603 km is still an improvement relative to the 654 km error for JTWC. A comparison between Table 17 and Table 15 shows that the cases randomly chosen for inclusion in the independent sample appear to have been slightly easier to forecast than

those in the dependent sample. Since the error characteristics of the two samples are different, it is likely that the sample sizes are too small.

TABLE 16

Decision tree selection of objective aids for the independent sample cases. The main diagonal contains the number of correct classifications by the tree.

		TRUE CLASS							
		RECR	TOTL	CLIM	XTRP	HPAC	CLIP	OTCM	NTCM
PREDICTED CLASS	RECR	1	3	3	6	2	4	4	2
	TOTL	0	0	0	0	0	0	0	0
	CLIM	1	0	0	0	0	3	0	2
	XTRP	5	0	1	2	0	2	0	0
	HPAC	0	0	0	0	0	0	0	0
	CLIP	0	0	0	0	0	0	0	0
	OTCM	4	2	2	1	3	1	7	3
	NTCM	4	2	3	6	5	4	9	11
	SUM	15	7	9	15	10	14	20	18
% CORRECT		6	0	0	13	0	0	35	61

TABLE 17

Overall mean and standard deviations of the 72-h forecast errors (km) for the independent sample as selected by the decision tree (TREE), if the BEST and WORST objective aid were always chosen , and the CLIP and JTWC forecasts. The JTWC values are for 97 cases compared to 108 cases for the others.

	TREE	BEST	WORST	CLIP	JTWC
Mean	603	298	1190	635	654
Std. Dev.	382	196	692	457	380

C. DISCUSSION

The decision tree method for selecting objective aids does have limited success in choosing the correct objective aid. The OTCM and NTCM are the models most frequently selected by the tree for both sample sets. These models should better handle anomalous tracks from a dynamical viewpoint and the OTCM is generally accepted as the overall best aid (Elsberry and Peak, 1986). Consequently, the inability to select the best aid is not serious if the second best aid turns out to be almost as good. Thus, a reduction in forecast errors by 11.2 % (7.2 %) for the dependent (independent) samples was achieved over the official JTWC forecast errors.

The selection of the zonal 700 mb wind EOF coefficients as the most important splitting parameters is indicative of the importance of the low-level winds in steering the cyclone. It is surprising that vertical wind shear is not found to be as important a parameter in choosing the optimum objective aid using the decision tree. In cases in which the tropical cyclone encounters strong upper-level forcing that shears off the top of the circulation, the vortex will continue to move with the low-level flow. These cases may not be handled well by the models because of the practice of entering a bogus vortex in the dynamical models (Fiorino, 1985) that extends through the entire troposphere. It is reasonable that in these cases in which wind shear is important that the wind EOF coefficients at lower levels play an increasingly dominant role as far as the tree algorithm is considered. However, the synoptic forcing parameters describing the vertical wind shear may not contribute to the decision tree because the dynamical models are not likely to be the optimum aid in these cases, since an unrealistic deep tropospheric bogus is inserted. In summary, the primary use of the vertical wind shear information seems to be in adjusting the dynamical model forecast tracks by the post-processing scheme described in Chapter IV.

VI. SUMMARY AND CONCLUSIONS

Vertical wind shear in the environment of tropical cyclones is investigated to determine the effects of such shear on storm motion. Wind fields derived from the U. S. Navy Global Band Analysis are used to compute the zonal and meridional components of vertical wind shear for the 400-700 mb, 250-400 mb and 250-700 mb levels on a 527 point grid around the tropical cyclone. Following Wilson (1984), these vertical shear fields are represented using empirical orthogonal functions (EOF). Schott (1985) demonstrated that EOF coefficients of zonal and meridional wind components at single levels can be used to represent the synoptic forcing of the surrounding wind fields on tropical cyclone motion. A dependent sample of 682 cases is selected for an EOF analysis of the wind-shear fields. Using a Monte Carlo selection technique, the number of eigenvectors chosen to represent true signals is 25 zonal and 35 meridional modes. Retaining this number of modes leads to explained variances ranging from 79 to 88 %.

The storms are stratified into five past-motion categories as proposed by Peak and Elsberry (1986). These categories are based on the storm's past speed and direction of motion. Means and standard deviations of the zonal and meridional wind-shear fields are constructed for each category. Because the majority of cases (497) move to the northwest (average direction of 301°), the other composites within the storm motion categories are compared to this category. The Student's t-test is used to indicate the statistical differences between the composite mean vertical wind shears at the gridpoints. The number of statistically different gridpoints at the 95 % confidence level range from 27 to 466 out of a possible 527 gridpoints. The largest (88) percentage of gridpoints with statistically different means occur for the deep-layer shear fields between the northwest and northeast past-motion categories. The northwest-moving cases are further subdivided into cross-track and along-track terciles. Statistically significant differences are found at up to 421 gridpoints for the left-turning minus right-turning storms within the northwest moving cases. This demonstrates that the vertical shears derived from operationally analyzed wind fields contain synoptic forcing information that is relevant to tropical cyclone motion.

A stepwise regression analysis is used to identify potential predictors to post-process the OTCM forecast tracks for 1982-1983. The set of potential predictors represent initial storm characteristics, forward and backward extrapolated tracks, and synoptic forcing from wind and wind-shear EOF coefficients. After screening, this set was reduced to 99 predictors. Only four wind-shear EOF predictors are selected compared to 18 wind-based EOF predictors. The regression equations are applied to the 24-, 48- and 72-h OTCM forecasts. For the dependent sample, the mean forecast error at 72 h is only 419 km. This is compared to 593 km for the unmodified OTCM and 631 km for the official JTWC forecasts. Thus, the vertical wind-shear EOF coefficients represent important information about the environment surrounding a tropical cyclone and, when used with other predictors in a regression analysis scheme, can improve the forecasts of operational tropical cyclone models. However, the scheme should be tested with independent data before operational implementation of these regression equations. At 72 h, the dependent sample used to generate the equations contained only 161 cases from 1982-1983. Predictors associated with independent cases may be different from those chosen in this study.

The wind-shear EOF coefficients were included in a decision tree that selects the optimum objective aid based on storm-related and synoptic parameters (Peak and Elsberry, 1987). The decision tree correctly selected the aid that produced the best 72-h forecast in 27 % (19 %) of the dependent (independent) cases. The tree depended almost entirely on the wind EOF coefficents at single levels as parameters to select among the aids. The lack of vertical wind-shear predictors used by the tree is disappointing but may be a result of the improper handling by all the models of cases with large wind shear. Thus, wind-shear predictors appear to be more useful when used in post-processing dynamic model forecast tracks.

In Wilson (1984), Schott (1985) and this study, a scalar EOF analysis was done. A vector analysis of the total wind and wind-shear fields may give additional insight into the synoptic forcing that results in anomalous storm tracks. With the preliminary success of these regression equations to adjust the OTCM forecast, this technique could be further developed for use with the NTCM. Additional synoptic parameters should also be investigated. The 12 or 24-h intensity changes and the radius of 30-kt winds are two such parameters that may play an important role in storm motion as a result of the interaction of the vortex and its environment.

LIST OF REFERENCES

Brand, S., C. A. Buenafe and H. D. Hamilton, 1981: Comparison of tropical cyclone motion and environmental steering. *Mon. Wea. Rev.*, **109**, 908-909.

Breiman, L., J. H. Friedman, R. A. Olshen and C. J. Stone, 1984: *Classification and Regression Trees.* Wadsworth International Group, Belmont, CA, 94002, 358 pp.

Chan, J. C. -L., 1985: Identification of the steering flow for tropical cyclone motion from objectively analyzed wind fields. *Mon. Wea. Rev.*, **113**, 106-116.

____, and W. M. Gray, 1982: Tropical cyclone movement and surrounding flow relationships. *Mon. Wea. Rev.*, **110**, 1354-1374.

____, W. M. Gray and S. Q. Kidder, 1980: Forecasting tropical cyclone turning motion from surrounding wind and temperature fields. *Mon. Wea. Rev.*, **108**, 778-792.

Dixon, W. J., and M. B. Brown, 1979: BMDP Biomedical Computer Program P-Series. University of California Press, Berkeley, CA, 367-460.

Dong, K., and C. J. Neumann, 1986: The relationship between tropical cyclone motion and environmental geostrophic flows. *Mon. Wea. Rev.*, **114**, 115-122.

Elsberry, R. L., and D. R. Frill, 1980: Statistical post-processing of dynamical tropical cyclone model track forecasts. *Mon. Wea. Rev.*, **108**, 1219-1225.

____, and J. E. Peak, 1986: An evaluation of tropical cyclone forecast aids based on cross-track and along-track components. *Mon. Wea. Rev.*, **114**, 147-155.

Fiorino, M., 1985: Operational numerical modeling of tropical cyclone motion. WMO International Workshop on Tropical Cyclones, Bangkok, Thailand. Tech. Document WMO/TD-No.74, A1-A9.

George, J. E., and W. M. Gray, 1976: Tropical cyclone motion and surrounding flow relationships. *J. Appl. Meteor.*, **15**, 1252-1264.

Gray, W. M., 1979: Hurricanes: their formation, structure and likely role in the tropical circulation. *Meteorology over the Tropical Oceans.* D. B. Shaw (Ed.), Royal Meteorological Society, Bracknell, Great Britain, 155-218.

Harrison, E. J., Jr., 1973: Three-dimensional numerical simulations of tropical systems utilizing nested finite grids. *J. Atmos. Sci.*, **30**, 1528-1543.

____, 1981: Initial results from the Navy two-way interactive nested tropical cyclone model. *Mon. Wea. Rev.*, **109**, 173-177.

____, and M. Fiorino, 1982: A comprehensive test of the Navy Nested Tropical Cyclone Model. *Mon. Wea. Rev.*, **110**, 645-650.

Hodge, W. T., and G. F. McKay, 1970: A computer program to select typhoon analogs and printout their descriptions including subsequent changes. *First Progress Report*, NAVWEARSCHFAC Project Order PO-90003, ESSA, Natl. Wea. Rec. Cen., Ashville, NC, 40 pp.

Hodur, R. M., and S. D. Burk, 1978: The Fleet Numerical Weather Central tropical cyclone model: Comparison of cyclic and one-way boundary conditions. *Mon. Wea. Rev.*, **106**, 1665-1671.

Hope, J. R., and C. J. Neumann, 1970: An operational technique for relating the movement of existing tropical cyclones to past tracks. *Mon. Wea. Rev.*, **98**, 925-933.

Hovermale, J. B., D. G. Marks, R. T. Chu, S. H. Scolnik and R. V. Jones, 1975: Experimental forecasts of hurricane movement with a limited area fine mesh grid. *Bull. Amer. Meteor. Soc.*, **7**, 29-38.

Jarrell, J. D., S. Brand and D. S. Nicklin, 1978: An analysis of western North Pacific tropical cyclone forecasting errors. *Mon. Wea. Rev.*, **106**, 925-937.

Jones, H., 1986: Comparison of western North Pacific tropical cyclone aids using storm-related and synoptic parameters. M. S. Thesis, Naval Postgraduate School, Monterey, CA, 140 pp.

Ley, G. W., and R. L. Elsberry, 1976: Forecasts of Typhoon Irma using a nested-grid model. *Mon. Wea. Rev.*, **104**, 1154-1161.

Lorenz, E. N.,1956: Empirical orthogonal functions and stastistical weather predictions. Department of Meteorology, Massachusetts Institute of Technology, Cambridge, MA, Scientific Report 1, Statistical Forecasting Project, 48 pp.

Naval Oceanography Command Center/Joint Typhoon Warning Center (NAVOCEANCOMCEN/JTWC), 1984: *1984 Annual Tropical Cyclone Report*, COMNAVMARIANAS Box 17, FPO San Francisco, CA, 219 pp.

Neumann, C. J., 1979: On the use of deep-layer mean geopotential height fields in statistical prediction of tropical cyclone motion. *Preprints. Sixth Conf. on Probability and Statistics in Atmosphere Sciences*, Banff, Amer. Meteor. Soc., 32-38.

____, 1985: The role of statistical models in the prediction of tropical cyclone motion. *Amer. Statistician*, **39**, 347-357.

____, and M. B. Lawrence, 1975: An operational experiment in the statistical-dynamical prediction of tropical cyclone motion. evaluation. *Mon. Wea. Rev.*, **103**, 665-673.

____, and J. M. Pelissier, 1981: Models for the prediction of tropical cyclone motion over the North Atlantic: An operational evaluation. *Mon. Wea. Rev.*, **109**, 522-538.

Peak, J. E., and R. L. Elsberry, 1982: A simplified stastical post-processing technique for adjusting tropical cyclone tracks. *Pap. Meteor. Res.*, **5**, 1-14.

____, and R. L. Elsberry, 1985: Objective selection of optimum tropical cyclone guidance using a decision-tree methodology. *16th Conf. on Hurricanes and Tropical Meteorology*, Amer. Meteor. Soc., Boston, MA, 97-98.

____, and R. L. Elsberry, 1986: Prediction of tropical cyclone turning and acceleration using empirical orthogonal function representations. *Mon. Wea. Rev.*, **114**, 156-164.

____, and R. L. Elsberry, 1987: Selection of optimum tropical cyclone motion guidance using an objective classification tree methodology. *Mon. Wea. Rev.*, (in press).

Pike, A. C., 1985: The use of meteorological data in the prediction of tropical cyclones. *Amer. Statistician*, **39**, 335-346.

Preisendorfer, R. W., and T. P. Barnett, 1977: Significance tests for empirical orthogonal functions. *Proc. 5th Conf. on Probability and Statistics in Meteorology and Atmospheric Sciences*, Amer. Meteor. Soc., Boston, MA, 169-172.

Renard, R. J., 1968: Forecasting the motion of tropical cyclones using a numerically derived steering current and its bias. *Mon. Wea. Rev.*, **96**, 453-469.

____, S. G. Colgan, M. J. Daley and S. K. Rinard, 1973: Forecasting the motion of North Atlantic tropical cyclones by the objective MOHATT scheme. *Mon. Wea. Rev.*, **101**, 206-214.

Riehl, H., W. H. Haggard and R. W. Sanborn, 1956: On the prediction of 24-hour hurricane motion. *J. Meteor.*, **13**, 415-420.

Sanders, F., and R. W. Burpee, 1968: Experiments in barotropic hurricane track forecasting. *J. Appl. Meteor.*, **7**, 313-323.

____, A. L. Adams, N. J. B. Gordon and W. D. Jensen, 1980: Further development of a barotropic operational model for predicting paths of tropical storms. *Mon. Wea. Rev.*, **108**, 642-654.

Schott, T. B., 1985: Applications of wind empirical orthogonal functions in tropical cyclone motion studies. M. S. Thesis, Naval Postgraduate School, Monterey, CA, 99 pp.

____, J. C. -L. Chan and R. L. Elsberry, 1987: Further applications of empirical orthogonal functions of wind fields for tropical cyclone motion studies. *Mon. Wea. Rev.*, (in press).

Shaffer, A. R., and R. L. Elsberry, 1982: A statistical climatological tropical cyclone track prediction technique using an EOF representation of the synoptic forcing. *Mon. Wea. Rev.*, **110**, 1945-1954.

Shapiro, L. J., and C. J. Neumann, 1984: On the orientation of grid systems for the prediction of tropical cyclone motion. *Mon. Wea. Rev.*, **112**, 188-198.

Tsui, T. L., 1984: A selection technique for tropical cyclone objective aids. *Preprints, 15th Conf. on Hurricanes and Tropical Meteorology*, Amer. Meteor. Soc., Boston, MA, 40-44.

——, and A. J. Truschke, 1985: Combined Confidence Rating System. *16th Conf. on Hurricanes and Tropical Meteorology*, Amer. Meteor. Soc., Boston, MA, 174-175.

Wilson, W. E., 1984: Forecasting of tropical cyclone motion using an EOF representation of wind forcing. M. S. Thesis, Naval Postgraduate School, Monterey, CA, 86 pp.

Xu, Y., and C. J. Neumann, 1985: A statistical model for the prediction of western North Pacific tropical cyclone motion (WPCLPR). NOAA Tech. Memo. NWS NHC 28, 30 pp.

INITIAL DISTRIBUTION LIST

		No. Copies
1.	Defense Technical Information Center Cameron Station Alexandria, VA 22304-6145	2
2.	Library, Code 0142 Naval Postgraduate School Monterey, CA 93943-5002	2
3.	Chairman (Code 63Rd) Department of Meteorology Naval Postgraduate School Monterey, CA 93943-5000	1
4.	Chairman (Code 68Tm) Department of Oceanography Naval Postgraduate School Monterey, CA 93943-5000	1
5.	Professor R. L. Elsberry (Code 63Es) Department of Meteorology Naval Postgraduate School Monterey, CA 93943-5000	5
6.	Professor C. -P. Chang (Code 63Cp) Department of Meteorology Naval Postgraduate School Monterey, CA 93943-5000	1
7.	LCDR Denis H Meanor 5317 East Blvd. N.W. Canton, OH 44718	2
8.	Director Naval Oceanography Division Naval Observatory 34th and Massachusetts Avenue NW Washington, DC 20390	1
9.	Commander Naval Oceanography Command NSTL Station Bay St. Louis, MS 39522	1
10.	Commanding Officer Naval Oceanographic Office NSTL Station Bay St. Louis, MS 39522	1
11.	Commanding Officer Fleet Numerical Oceanography Center Monterey, CA 93943-5000	1
12.	Commanding Officer Naval Ocean Research and Development Activity NSTL Station Bay St. Louis, MS 39522	1
13.	Commanding Officer Naval Environmental Prediction Research Facility Monterey, CA 93943-5000	1

14.	Chairman, Oceanography Department U.S. Naval Academy Annapolis, MD 21402	1
15.	Chief of Naval Research 800 N. Quincy Street Arlington, VA 22217	1
16.	Office of Naval Research (Code 420) Naval Ocean Research and Development Activity 800 N. Quincy Street Arlington, VA 22217	1
17.	Commanding Officer Naval Eastern Oceanography Center Naval Air Station Norfolk, VA 23511	1
18.	Director Joint Typhoon Warning Center Box 17 FPO San Francisco, CA 96630	1
19.	Commanding Officer Naval Oceanographic Command Center, Guam Box 12 FPO San Francisco, CA 96630	1
20.	Mr. and Mrs. Howard A. Meanor 5317 East Blvd. N.W. Canton, OH 44718	1
21.	Mr. and Mrs. John Reed 4821 Keane Dr. Carmichael, CA 95608	1